# Molecular Cleft Reactivity and Conformational Properties of Skeletally Stabilized Triphosphazanes

**Susan M. Young, Abbas Tarassoli,[1a] Joseph M. Barendt,[1b] Christopher A. Squiers,[1c] Francoise Barthelemy, Riley Schaeffer, R. Curtis Haltiwanger, and Arlan D. Norman***

Department of Chemistry and Biochemistry, University of Colorado, Boulder, Colorado 80309

*Received December 17, 1993**

Regioselective reactivity, molecular cleft selectivity, and conformational properties have been examined in the skeletally stabilized triphosphazanes $C_6H_4N_2[P(NEt_2)_2]_2PNEt_2$ (**3**), $C_6H_4N_2[P(S)(NEt_2)_2]_2PNEt_2$ (**4**), $C_6H_4N_2[P(S)(NEt_2)_2]_2PCl$ (**5**), and $C_6H_4N_2[P(S)(NEt_2)_2]_2P(S)NEt_2$ (**9**) and in a series of new derivatives. **3** is oxidized/coordinated regioselectively by $O_3$, Se, $PhN_3$, and $BH_3$ to $C_6H_4N_2[P(O)(NEt_2)_2]_2PNEt_2$ (**10**) and $C_6H_4N_2[P(O)(NEt_2)_2]_2P(O)NEt_2$ (**11**), $C_6H_4N_2[P(Se)(NEt_2)_2]_2PNEt_2$ (**12**), $C_6H_4N_2[P(NPh)(NEt_2)_2]_2PNEt_2$ (**13**), and $C_6H_4N_2[P(BH_3)(NEt_2)_2]_2PNEt_2$ (**14**), respectively. **4** reacts selectively with $HBF_4$, $CF_3CO_2H$, and $H_3PO_4$ to form the endo-phosphorus-substituted $C_6H_4N_2[P(S)(NEt_2)_2]_2PF$ (**18**), $C_6H_4N_2[P(S)(NEt_2)_2]_2POC(O)CF_3$ (**19**), and $C_6H_4N_2[P(S)(NEt_2)_2]_2POP(O)(OH)_2$ (**20**). Quantitative MeI quaternization or $BH_3$ coordination of **4** yields $\{C_6H_4N_2[P(S)(NEt_2)_2]_2P(CH_3)NEt_2\}I$ (**16**) or $C_6H_4N_2[P(S)(NEt_2)_2]_2P(BH_3)NEt_2$ (**15**). **5** reacts selectively with alcohols MeOH, EtOH, and i-PrOH (but is inert toward t-BuOH) to form $C_6H_4N_2[P(S)(NEt_2)_2]_2POR$ [R = Me (**21**), Et (**22**), i-Pr (**23**)] and with $BH_3$ to form $C_6H_4N_2[P(S)(NEt_2)_2]_2PH$ (**25**) and its adduct $C_6H_4N_2[P(S)(NEt_2)_2]_2PH(BH_3)$ (**24**). New triphosphazanes **10-16** and **18-25** are characterized by spectral data. Structures of **9**, **12**, and **16** are determined by X-ray crystallography: **9**, orthorhombic, *Aba*2, $a = 23.111(4)$ Å, $b = 21.324(5)$ Å, $c = 14.609(3)$ Å, $V = 7200(2)$ Å$^3$, $Z = 8$, $R = 0.042$, $R_w = 0.045$; **12**, orthorhombic, *Pbca*, $a = 14.975(6)$ Å, $b = 18.894(7)$ Å, $c = 24.524(8)$ Å, $V = 6939(3)$ Å$^3$, $Z = 8$, $R = 0.053$, $R_w = 0.058$; **16**, orthorhombic, $C222_1$, $a = 10.885(4)$ Å, $b = 20.78(2)$ Å, $c = 36.31(2)$ Å, $V = 8214(9)$ Å$^3$, $Z = 8$, $R = 0.048$, $R_w = 0.050$. Variable-temperature $^{31}P\{^1H\}$ NMR spectra of **3-5**, **10**, **11**, **15**, **16**, and **20** and of the known $C_6H_4N_2[P(S)(NEt_2)_2]_2PNH_2$ (**6**), $C_6H_4N_2[P(S)(NEt_2)_2]_2PN_3$ (**7**), and $C_6H_4N_2[P(S)(NEt_2)_2]_2P(O)H$ (**8**) show that rotation around skeletal exo P-N bonds is unrestricted to below -90 °C; only **9** and **11** freeze to unsymmetrical conformations at low temperatures. Rotation of the endo $(CH_3CH_2)_2N$- group in the molecular cleft of **3** is unrestricted to -90 °C; in **16** the group freezes to an unsymmetrical conformation below -40 °C. Potential impacts of the observed reaction selectivity and conformational properties on oligomeric/polymeric phosphazane structure and reactivity are discussed.

## Introduction

Skeletally stabilized phosphazane oligomers and polymers containing alternating skeletal phosphorus and nitrogen atoms bridged at adjacent nitrogen atoms by 1,2-$C_6H_4$ groups have been the subject of several recent studies.[2-7] From 1,2-$(NH_2)_2C_6H_4/RPCl_2$ (R = Me, Ph) condensation[4-6] or 1,2-$(NH_2)_2C_6H_4/RP(NEt_2)_2$ (R = Me, Et, Ph) transamination[4-7] reactions, polymers (**1**), linear oligomers, and cyclic crown type cyclo dimers (**1**; $n = 2$)[4-6,8] and trimers (**1**; $n = 3$)[8] are formed. These new skeletally stabilized extended phosphazanes lead to basic questions about reactivity and molecular structure. Since

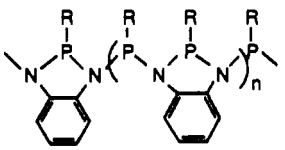

**1**

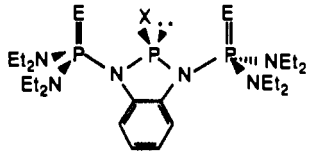

**3** (X = $Et_2N$, E = lone pair)
**4** (X = $Et_2N$, E = S)
**5** (E = S, X = Cl)

it is known that diphosphazane condensation reactions can occur with a high degree of stereoselectivity,[9] it is possible that higher phosphazanes can also form stereoregularly. Second, although diphosphazane conformational properties have been examined,[10-20] little is known about conformations in higher phosphazanes.

* Abstract published in *Advance ACS Abstracts*, June 1, 1994.

(1) Present address: (a) Department of Chemistry, Shahid Chamran University, Ahwaz, Iran. (b) Callery Chemical Co., P.O. Box 429, Pittsburgh, PA 15230. (c) Smithkline Beechum, P.O. Box 1539, L-950, King of Prussia, PA 19406.

(2) (a) Barendt, J. M.; Haltiwanger, R. C.; Norman, A. D. *J. Am. Chem. Soc.* **1986**, *108*, 3127. (b) Barendt, J. M.; Haltiwanger, R. C.; Norman, A. D. *Inorg. Chem.* **1989**, *28*, 2334. (c) Bent, E. G.; Schaeffer, R.; Haltiwanger, R. C.; Norman, A. D. *Inorg. Chem.* **1990**, *29*, 2608.

(3) (a) Barendt, J. M.; Haltiwanger, R. C.; Norman, A. D. *Inorg. Chem.* **1986**, *25*, 4323. (b) Barendt, J. M.; Haltiwanger, R. C.; Squier, C. A.; Norman, A. D. *Inorg. Chem.* **1991**, *30*, 2342.

(4) Bent. E. G.; Barendt, J. M.; Haltiwanger, R. C.; Norman, A. D. *Inorganic and Organometallic Polymers*; ACS Symposium Series 360; American Chemical Society: Washington, DC, 1988; p 303.

(5) (a) Barendt, J. M.; Bent, E. G.; Haltiwanger, R. C.; Norman, A. D. *J. Am. Chem. Soc.* **1989**, *111*, 6883. (b) Barendt, J. M.; Bent, E. G.; Young, S. M.; Haltiwanger, R. C.; Norman, A. D. *Inorg. Chem.* **1991**, *30*, 325.

(6) Norman, A. D.; Bent, E. G.; Haltiwanger, R. C.; Prout, T. R. *Phosphorus Sulfur*, **1989**, *41*, 63.

(7) Bent, E. G.; Haltiwanger, R. C.; Norman, A. D. *Inorg. Chem.* **1990**, *29*, 4310.

(8) Young, S. M.; Imiolczyk, T. M.; Haltiwanger, R. C.; Norman, A. D. Submitted for publication.

(9) (a) Hill. T. G.; Haltiwanger, R. C.; Norman, A. D. *Inorg. Chem.* **1985**, *24*, 3499. (b) Prout, T. R.; Imiolczyk, T. W.; Haltiwanger, R. C.; Hill, T. G.; Norman, A. D. *Inorg. Chem.* **1992**, *31*, 215.

(10) Keat, R. *Top. Curr. Chem.* **1982**, *102*, 89.

(11) Prout, T. R.; Imiolczyk, T. W.; Barthelemy, F.; Young, S. M.; Haltiwanger, R. C.; Norman, A. D. *Inorg. Chem.* **1994**, *33*, 1783.

(12) Keat, R.; Manojlovic'-Muir, L.; Muir, K. W.; Rycroft, D. S. *J. Chem. Soc., Dalton Trans.* **1981**, 2192 and references cited therein.

(13) Cross, R. J.; Green, T. H. Keat, R. *J. Chem. Soc., Dalton Trans.* **1976**, 1424.

(14) Colquhoun, I. J.; McFarlane, W. *J. Chem. Soc., Dalton Trans.* **1977**, 1674.

(15) Harvey, D. A.; Keat, R.; Keith, A. N.; Muir, K. W.; Rycroft, D. S. *Inorg. Chim. Acta* **1979**, *34*, L201.

(16) Rudolph, R. W.; Newmark, R. A. *J. Am. Chem. Soc.* **1970**, *92*, 1195.

(17) (a) Ebsworth, E. A. V.; Rankin, D. W. H.; Wright, J. G. *J. Chem. Soc., Dalton Trans.* **1977**, 2348. (b) Ebsworth, E. A. V.; Rankin, D. W. H.; Wright, J. G. *J. Chem. Soc., Dalton Trans.* **1979**, 1065.

(18) Hägele, G.; Harris, R. K.; Wazeer, M. I. M.; Keat, R. *J. Chem. Soc., Dalton Trans.* **1986**, 1974.

0020-1669/94/1333-2748$04.50/0 

Finally, there is insufficient information to assess the reactivity and/or accessibility of nonterminal skeletal phosphorus centers to P–X substituent replacement, Lewis acid coordination, or oxidation [e.g. P(III) to P(V)]. The latter question is further complicated by the fact that these skeletally stabilized systems contain two types of phosphorus environments, bridge RP and phosphadiazole RP units, which could possess significantly different reactivities.

A triphosphazane unit, such as **2A** or **2B**, is a minimum-sized phosphazane that can yield representative information about extended skeletal phosphazane conformational properties around,

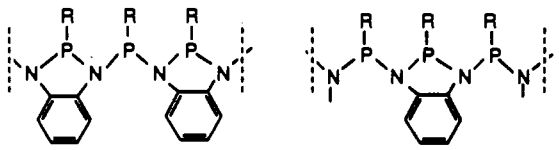

**2A**



**2B**

or reactivity at, the RP centers. From recent studies, one such triphosphazane is available, $C_6H_4N_2[P(NEt_2)_2]_2PNEt_2$ (**3**, X = $Et_2N$), a species which could model a central phosphadiazole type triphosphazane (**2B**).[2b,21] In preliminary studies, **3** exhibited highly regioselective oxidation by $S_8$ at the exo vs endo phosphorus atoms.[3] Further, the disulfide $C_6H_4N_2[P(S)(NEt_2)_2]_2PNEt_2$ (**4**) and chloro-substituted derivative $C_6H_4N_2[P(S)(NEt_2)_2]_2PCl$ (**5**) showed restricted reactivity at the endo phosphorus, which was attributed to the existence of a protective molecular cleft at the central (endo) phosphorus site. We have now extended our studies of triphosphazanes in this series; the results are described below.

## Experimental Section

**Apparatus and Materials.** Phosphorus-31, $^{11}B$, and $^{19}F$ NMR spectra were obtained on a Varian Gemini or a VXR300S spectrometer at 121.4, 96.2, and 292.2 Hz, respectively. $^{31}P$ NMR spectra were also obtained with JEOL FX-90Q and Bruker WM-250 spectrometers at 36.5 and 101.2 MHz. $^1H$ NMR spectra were obtained on JEOL FX-90Q (90 MHz) and Varian Gemini-300 or VXR300S (300 MHz) NMR spectrometers. $^{31}P$, $^1H$, $^{11}B$, and $^{19}F$ chemical shifts downfield from 85% $H_3PO_4$ (external), $Me_4Si$ (internal), $BF_3OEt_2$ (external), and $CF_3CO_2H$ (external), respectively, are reported as positive (+$\delta$). IR spectra (4000–400 $cm^{-1}$) were obtained using a Beckman 4250 or an IBM IR/32 Type 9132 spectrometer. Mass spectra were obtained at 70 eV with a Varian MAT-CH5 or a VG Analytical 7070 EQ-HF spectrometer. Mass spectral data refer to the major peak of the respective envelope. Chemical ionization ($CI^+$ and $CI^-$) was achieved using isobutane as the ionizing gas. Exact mass analyses were referenced to perfluorokerosene. Ozonolyses were carried out in a Welsbach Ozonator Model T-408 operating at 90 V. X-ray diffraction data were collected on a Nicolet P3/F automated diffractometer equipped with a graphite monochromator and low-temperature attachment. All manipulations were carried out using standard vacuum-line, glovebag, or Schlenk techniques under dry $N_2$.[22]

Flash chromatography was carried out as described by Still et al.[23] A 650- or 450-mL column was packed (15 cm) with silica gel 60 (230–400 mesh). Compounds were eluted with the necessary solvent mixture under $N_2$ pressure at 5 cm/min.

Elemental analyses were performed by Huffman Laboratories Inc., Golden, CO, and Desert Analytics, Tuscon, AZ.

1,2-$(NH_2)_2C_6H_4$ (Aldrich) was recrystallized from toluene and sublimed. $CF_3CO_2H$ (Aldrich) was stored over 13-Å molecular sieves. $CH_3I$ was distilled from $CaH_2$. Toluene (over Na/benzophenone or $CaH_2$) and $CH_2Cl_2$ ($CaH_2$) were distilled before use. $H_3PO_4$ was dried with $P_4O_{10}$. Silica gel (EM Science), KBr (Baker, oven dried), Se (laboratory supply), $HBF_4$ (85% in $Et_2O$ complex, Aldrich), $BH_3$·THF (1.0 M in THF, Aldrich), petroleum ether, ethyl acetate, and deuterated solvents were used as received. PhIO (Aldrich) and $Me_3NO$ (Aldrich) were sublimed before use. $B_2H_6$,[24] $PhN_3$,[25] $C_6H_4N_2[P(NEt_2)_2]_2PNEt_2$ (**3**),[2b] $C_6H_4N_2[P(S)(NEt_2)_2]_2PNEt_2$ (**4**),[2b] $C_6H_4N_2[P(S)(NEt_2)_2]_2PCl$ (**5**),[2b] $C_6H_4N_2[P(S)(NEt_2)_2]_2PNH_2$ (**6**),[2b] $C_6H_4N_2[P(S)(NEt_2)_2]_2PN_3$ (**7**),[2b] $C_6H_4N_2[P(S)(NEt_2)_2]_2P(O)H$ (**8**),[2b] and $C_6H_4N_2[P(S)Ph_2]_2P(S)NEt_2$ (**9**)[2b] were prepared as described previously.

**Reactions of $C_6H_4N_2[P(NEt_2)_2]_2PNEt_2$ (3). (A) With Ozone. $C_6H_4N_2[P(O)(NEt_2)_2]_2PNEt_2$ (10) and $C_6H_4N_2[P(O)(NEt_2)_2]_2P(O)NEt_2$ (11).** To $C_6H_4N_2[P(NEt_2)_2]_2PNEt_2$ (**3**) (20 mmol) in 120 mL of $CH_2Cl_2$ in a Schlenk tube at 10–12 °C was added $O_3$ as $O_3/O_2$ at 8 psi. Samples were taken every 3 min for $^{31}P$ NMR analysis. After 42 min, resonances were present at $\delta$ 13.7 (d, area 2, $^2J_{PNP}$ = 51.3 Hz] and 97.9 (t, area 1) and at $\delta$ 11.3 (d, area 2, $^2J_{PNP}$ = 16.5 Hz) and 19.2 (t, area 1) due to **10** and **11**, respectively (**10**:**11** = 2:1). Attempts to separate the mixture by crystallization or column chromatography failed. No distinguishable change in the mixture composition was observed after 2 weeks at 25 °C. Conditions under which **10** formed without **11** were not found.

Addition of $O_3$ to **3** in $CH_2Cl_2$ at 10–12 °C (as above) for 100 min yielded **11** quantitatively. **11** crystallized from $CH_2Cl_2$ (mp 109–111 °C, yield 97%). MS: $M^+$ *m/e* 605. IR (KBr, $cm^{-1}$): 2978 (s), 2935 (s), 2875 (s), 1680 (w), 1593 (s), 1488 (vs), 1465 (m), 1382 (m), 1360 (w), 1332 (w), 1302 (w), 1255 (w), 1232 (s), 1211 (s), 1192 (s), 1170 (w), 1120 (vs), 1100 (m), 1065 (m), 1035 (w), 1008 (w), 962 (vs), 942-(w), 918 (m), 908 (vs), 794 (vs), 755 (vs), 735 (m), 716 (vs), 694 (vs), 668 (s), 562 (w), 532 (m), 502 (m), 460 (m). Mol wt: calcd for $C_{26}H_{54}N_7O_3P_3$, 605.357 94; found (exact mass MS), 605.357 88. Because samples were routinely contaminated with traces of $H_2O$ which we were unable to remove completely, satisfactory chemical elemental analyses were not obtained. $^{31}P\{^1H\}$ NMR (toluene-$d_8$, 27 °C): $AX_2$ pattern,[26] $\delta$ 10.5 [d, area 2, $^2J_{PP}$ = 14.7 Hz; P(1), P(3)], 19.0 [t, area 1, P(2)]. $^{31}P\{^1H\}$ NMR (EtOH), 27 °C): $\delta$ 11.0 (d, area 2, *J* = 17.1 Hz), 18.6 (t, area 1). $^1H$ NMR (toluene-$d_8$): $\delta$ 7.23–6.92 (m, area 4; $C_6H_4$), 3.26–2.84 (m, area 20; $CH_2$), 1.00 (m, area 30; $CH_3$).

**11** reacted slowly with $H_2O$, during 6 h, to form a mixture of so-far-uncharacterized products.

**(B) With Other [O] Oxidants.** **3** with excess PhIO or $Me_3NO$ in refluxing benzene for 20 h showed no reaction.

**(C) With Selenium. $C_6H_4N_2[P(Se)(NEt_2)_2]_2PNEt_2$ (12).** **3** and excess Se in toluene were refluxed for 12 h. $^{31}P$ NMR spectral analysis showed only **12**. Recrystallization from toluene yielded **12** (mp 128–129 °C, yield >90%). $^{31}P\{^1H\}$ NMR ($C_6H_6$, 27 °C): $\delta$ 99.7 [d, area 2, $^2J_{PNP}$ = 68.4 Hz; P(1), P(3)], 63.0 [t, area 1; P(1)]; $J_{PSe}$ = 391 Hz. $^{31}P\{^1H\}$ VT NMR (toluene-$d_8$): $^2J_{PNP}$, Hz (temp, °C): 68.4 (25), 68.2 (00), 68.1 (–30), 68.3 (–60), 68.0 (–90). $^1H$ NMR ($C_6D_6$): $\delta$ 7.54 (m, area 2; $C_6H_4$ ortho), 6.86 (m, area 2; $C_6H_4$ ortho), 3.40 (m, area 4; exo $CH_2CH_3$), 3.13 (m, area 12; exo $CH_2CH_3$), 2.82 (m, area 4; endo $CH_2CH_3$), 0.9–1.2 (m, area 30; $CH_3$). IR (KBr, $cm^{-1}$): 2924 (m), 1586 (s), 1482 (vs), 1377 (vs), 1331 (w), 1293 (w), 1250 (vs), 1200 (s), 1165 (vs), 1115 (w), 1061 (vs), 945 (vs), 883 (vs), 794 (vs), 741 (s), 691 (w), 579 (m), 509 (m), 475 (m), 428 (w). MS: $M^+$ *m/e* 717. Anal. Calcd for $C_{26}H_{54}N_7P_3Se_2$: C, 43.64; H, 7.55; N, 13.69. Found: C, 44.64; H, 7.85; N, 13.04.

**(D) With $PhN_3$. $C_6H_4N_2[P(NPh)(NEt_2)_2]_2PNEt_2$ (13).** **3** and $PhN_3$ [(2–3):1 mole ratio] in toluene were combined at 25 °C; reaction occurred immediately. $^{31}P$ NMR spectra showed **13** with only traces of unidentified materials. Removal of toluene in vacuo yielded **13** as an oil (>90%), which we were unable to purify completely by crystallization or column chromatography. $^{31}P\{^1H\}$ NMR ($C_6H_6$): $\delta$ 99.1 [t, area 1, $^2J_{PNP}$ = 47.6 Hz; P(2)], 32.9 [d, area 2; P(1), P(3)].

**(E) With $BH_3$·THF. $C_6H_4N_2[P(BH_3)(NEt_2)_2]_2PNEt_2$ (14).** $BH_3$·THF (excess) was added under $N_2$ to a solution of **3** in THF at room temperature, and the mixture was stirred overnight. The $^{31}P$ NMR spectrum showed only **14**. The reaction solution was concentrated in vacuo. **14** precipitated upon cooling to 0 °C and was recrystallized from toluene (mp 152–154 °C, yield 92%). $^1H$ NMR ($C_6D_6$): $\delta$ 7.57 (m, area 2; $C_6H_4$ ortho), 6.84 (m, area 2; $C_6H_4$ meta), 3.40 (m, area 20; $CH_2CH_3$), 1.30 (br m, area 6; $PBH_3$), 1.05 (t, area 12, $^3J_{HH}$ = 7.08 Hz; exo $CH_2CH_3$), 0.93 (t, area 6, $^3J_{HH}$ = 7.08 Hz; endo $CH_2CH_3$), 0.91 (t, area 12, $^3J_{HH}$ = 7.08 Hz;

(19) Bulloch, G.; Keat, R.; Rycroft, D. S.; Thompson, D. G. *Org. Magn. Reson.* **1979**, *12*, 708.
(20) Chen, H.-J.; Barendt, J. M.; Haltiwanger, R. C.; Hill, T. G.; Norman, A. D. *Phosphorus Sulfur* **1986**, *26*, 155.
(21) Moskva, V. V.; Kuliev, A. K.; Akhmedzade, D. A.; Pudovik, M. A.; Sakhnovskaya. *J. Gen. Chem. USSR (Engl. Transl.)* **1985**, *55*, 834.
(22) Shriver, D. F.; Drezdzon, M. A. *The Manipulation of Air-Sensitive Compounds*, 2nd ed.; McGraw Hill: New York, 1986.
(23) Still, W. C.; Kahn, M.; Mitra, A. *J. Org. Chem.* **1978**, *43*, 2923.
(24) Norman. A. D.; Jolly, W. L. *Inorg. Synthesis* **1968**, *11*, 15.
(25) Lindsay, R. O.; Allen, C. F. H. *Organic Syntheses*; Wiley: New York, 1955; Collect. Vol. III, p 710.
(26) Abraham, R. J. *The Analysis of High Resolution NMR Spectra*; Elsevier Publishing Co.: New York, 1971.

exo $CH_2CH_3$). $^{31}P\{^1H\}$ NMR (toluene-$d_8$, 27 °C): δ 100.3 [t, area 1, $^2J_{PNP}$ = 59.3 Hz; $P(NEt_2)$], 94.0 [br m, area 2; $P(BH_3)$]. $^{31}P\{^1H\}$ VT NMR (toluene-$d_8$): 70 °C, δ 101.3 [t, area 1, $^2J_{PNP}$ = 61.6 Hz; P(1), P(3)], 95.4 [d of q, area 2, $^1J_{PB}$ = 84.9 Hz; P(2)]; −90 °C, δ 98.4 (t, area 1, $^2J_{PNP}$ = 55.1 Hz), 90.0 (br d, area 2). $^2J_{PNP}$, Hz (temp, °C): 59.7 (100), 60.7 (90), 60.3 (80), 61.0 (70), 60.1 (60), 60.3 (50), 60.1 (40), 59.9 (30), 59.9 (25), 59.5 (0), 59.2 (−20), 58.2 (−40), 57.6 (−60), 55.9 (−80), 55.1 (−90). $^{11}B\{^1H\}$ NMR (toluene-$d_8$): δ −33.4 (d, $^1J_{BP}$ = 87.9 Hz); from $^1H$-coupled spectrum, d of q, $^1J_{BH}$ = 122 Hz. Anal. Calcd for $C_{26}H_{60}B_2N_7P_3$: C, 53.33; H, 10.26; N, 16.75. Found: C, 53.52; H, 10.48; N, 16.37. MS ($CI^+$), $M^+$ *m/e* (% rel int): 585 (5). IR (KBr, $cm^{-1}$): 3426 (w), 3060 (w), 2974 (vs), 2934 (s), 2870 (s), 2390 (vs), 2281 (w), 1586 (w), 1483 (vs), 1380 (vs), 1349 (m), 1332 (s), 1291 (m), 1251 (vs), 1202 (vs), 1178 (vs), 1119 (m), 1076 (s), 1028 (vs), 986 (m), 946 (vs), 890 (s), 866 (s), 842 (m), 797 (s), 738 (vs), 691 (s), 674 (m), 603 (w), 505 (m), 481 (m).

**Reactions of $C_6H_4N_2[P(S)(NEt_2)_2]_2PNEt_2$ (4). (A) With $B_2H_6$ and $BH_3$·THF. $C_6H_4N_2[P(S)(NEt_2)_2]_2P(BH_3)NEt_2$ (15).** $B_2H_6$ (0.13 mmol) was condensed onto **4** (0.065 mmol) in toluene-$d_8$, and the mixture was warmed to 25 °C. The $^{31}P$ NMR spectrum exhibited resonances from **15** and uncoordinated **4** (mole ratio **15**:**4** = 1.3:1). The $^{11}B\{^1H\}$ NMR spectrum showed singlet resonances from **15** and unreacted $B_2H_6$. $^{31}P\{^1H\}$ NMR (toluene-$d_8$): δ 108 (br s, area 1; $PBH_3$), 66.4 (d, area 2, $^2J_{PNP}$ = 34.0 Hz; P═S). $^{11}B\{^1H\}$ NMR (toluene-$d_8$): δ −33.8 (br s).

Measured quantities of $BH_3$·THF were added under $N_2$ to a solution of **4** in toluene-$d_8$ or THF in mole ratios of (0.5–10):1. Solutions were allowed to reach equilibrium at 20 °C (NMR probe temperature), and the **15**:**4** ratios were determined by integration of the $^{31}P$ NMR spectra. Typical reaction conditions are as follows. [$BH_3$·THF], [**4**], [THF] initial molar concentrations (solvent), **15**:**4** equilibrium ratio: (1) 0.121, 0.235, 12.3 (THF), 0.14:1; (2) 0.189, 0.161, 12.3 (THF), 0.22:1; (3) 0.343, 0.0850, 4.23 (THF), 1.1:1; (4) 0.857, 0.142, 12.3 (THF), 0.71:1; (5) 0.814, 0.0821, 12.3 (toluene), 0.58:1; (6) 0.471, 0.0456, 5.82 (toluene), 1.34:1. The $^{11}B\{^1H\}$ NMR spectrum showed singlet resonances from unreacted $BH_3$·THF and **15**. Removal of solvent and $BH_3$·THF in vacuo resulted in complete conversion of **15** to **4**.

**(B) With $CH_3I$. $\{C_6H_4N_2[P(S)(NEt_2)_2]_2P(CH_3)NEt_2\}I$ (16).** $CH_3I$ (0.2 mL, 3.2 mmol) was syringed into a solution of **3** (0.974 g, 1.6 mmol) in $CH_2Cl_2$ at 25 °C. Reaction occurred slowly; in 18 h the $^{31}P\{^1H\}$ NMR spectrum showed $AB_2$[19] pattern resonances assigned to **16** along with those of **3** (**16**:**3** = 2:1). Reaction was complete in 36 h. The solution contained mainly **16** along with minor amounts of **3** and $C_6H_4N_2[P(S)(NEt_2)_2]_2P(O)H$ (**8**) (<5%). Removal of solvent in vacuo and separation of **16** by flash column chromatography (95% $CH_2Cl_2$/MeOH), followed by recrystallization from toluene yielded pure **16** (mp 127–130 °C, yield ≥90%). $^{31}P\{^1H\}$ NMR ($CD_2Cl_2$, 27 °C): δ 65.7 (d, area 2, $^2J_{PNP}$ = 35.5 Hz; P═S), 62.1 (t, area 1; $PCH_3$). $^{31}P\{^1H\}$ VT NMR ($CD_2Cl_2$) $^2J_{PNP}$, Hz (temp, °C): 35.5 (25), 35.9 (0), 36.2 (−20), 36.1 (−40), 36.7 (−60), 37.0 (−80), 37.2 (−90). $^1H$ NMR ($CD_2Cl_2$): δ 7.8 (m, area 2; $C_6H_4$ ortho), 7.2 (m, area 2; $C_6H_4$ meta), 3.5 (m, area 4; endo $CH_2CH_3$), 3.2 (m, area 16; exo $CH_2CH_3$), 3.18 (d, area 3, $^2J_{HP}$ = 15.6 Hz; $PCH_3$), 1.36 (t, area 6, $^3J_{HH}$ = 7.08; endo $CH_2CH_3$), 1.26 (t, area 12, $^3J_{HH}$ = 7.08; exo $CH_2CH_3$), 1.01 (t, area 12, $^3J_{HH}$ = 7.08; exo $CH_2CH_3$). MS (FAB): $(M-I)^+$ *m/e* 636. IR (KBr, $cm^{-1}$): 3421 (w), 2973 (s), 2933 (s), 2874 (s), 1585 (w), 1474 (vs), 1382 (s), 1341 (m), 1319 (m), 1294 (m), 1227 (s), 1202 (vs), 1164 (vs), 1114 (s), 1060 (m), 1027 (s), 990 (m), 929 (vs), 896 (s), 805 (m), 763 (m), 723 (vs), 697 (m), 664 (m), 643 (w), 597 (w), 514 (m), 466 (m). Anal. Calcd for $C_{27}H_{57}N_7P_3S_2I$: C, 42.46; H, 7.47; N, 12.84. Found: C, 44.51; H, 7.64; N, 11.77.

In sealed NMR tube reactions ($CH_3I$:**4** = 3.5:1) spectral evidence for $C_6H_4N_2[P(S)(NEt_2)_2]_2PI$ (**17**) was seen (ratio **16**:**17** = 2:1). $^{31}P\{^1H\}$ NMR ($CD_2Cl_2$): δ 146.4 (t, area 1, $^2J_{PNP}$ = 64.5 Hz; *P*I), 66.9 (d, area 2; P═S). Addition of $HNEt_2$ to the solution containing **16** and **17** resulted in complete conversion of **17** to **4**.

**(C) With Se.** **4** showed no reaction with Se (in toluene solution) or KSeCN (in $CH_3CN$ solution) at temperatures from 25 to 110 °C.

**(D) With $HBF_4$. $C_6H_4N_2[P(S)(NEt_2)_2]_2PF$ (18).** $HBF_4$ (85%) (13.0 μL, 0.08 mmol) was syringed into a solution of **3** (0.049 g, 0.08 mmol) in THF at −80 °C. Reaction occurred immediately. Removal of THF in vacuo yielded an oil, which we were unable to purify by crystallization or column chromatography. $^{31}P\{^1H\}$ NMR (THF-$d_8$): δ 127.8 (d of t, area 1, $^1J_{PF}$ = 1184 Hz, $^2J_{PNP}$ = 54.7 Hz; *P*F), 66.4 (d, area 2; P═S). $^{19}F$ NMR (THF-$d_8$): δ 23.4 (d, $^1J_{FP}$ = 1184 Hz). Mol wt: calcd for $C_{22}H_{44}FN_6P_3S_2$, 568.2266; found (EI+, exact mass), *m/e* 568.2278. MS ($EI^+$), $M^+$ *m/e* (% rel int): 568 (12). The $^{11}B$ NMR spectrum showed a broad resonance at δ 0.5 attributable to $Et_2NH{\cdot}BF_3$.

**(E) With $CF_3CO_2H$. $C_6H_4N_2[P(S)(NEt_2)_2]_2PO_2CCF_3$ (19).** $CF_3CO_2H$ (0.09 mL, 1.2 mmol) was syringed into **4** (0.463 g, 0.75 mmol) in $CH_2Cl_2$ at 25 °C. The $^{31}P\{^1H\}$ NMR spectrum exhibited resonances from **18** and minor resonances from **8** (<15% spectral area). Removal of $CH_2Cl_2$ in vacuo yielded an uncrystallizable oil. Mol wt: calcd for $C_{24}H_{44}F_3N_6O_2P_3S_2$, 662.2132; found (EI+, exact mass), 662.2161. MS ($EI^+$), $M^+$ *m/e* (% rel int): 662 (3). $^{31}P\{^1H\}$ NMR ($C_6D_6$): δ 119.7 (t, area 1, $^2J_{PP}$ = 70.7 Hz; $PCO_2CF_3$), 66.6 (d, area 2; P═S). $^{19}F$ NMR ($C_6D_6$): δ 2.1 (s).

**(F) With $H_3PO_4$. $C_6H_4N_2[P(S)(NEt_2)_2]_2POP(O)(OH)_2$ (20).** A two-phase mixture of **4** (0.308 g, 0.50 mmol) and excess $H_3PO_4$ (>98% $H_3PO_4$) in $CH_2Cl_2$ at 25 °C was stirred for 0.5 h. The $CH_2Cl_2$ solution was decanted from any unreacted acid. The $^{31}P$ NMR spectrum showed **20** and **8**. Removal of $CH_2Cl_2$ in vacuo yielded **20** as an oil (>85%), which we were unable to purify by crystallization or column chromatography. $^{31}P\{^1H\}$ NMR ($CD_2Cl_2$, 27 °C): δ 113.2 (t of d, area 1, $^2J_{PNP}$ = 67.5 Hz, $^2J_{POP}$ = 20.6 Hz; $POP(O)(OH)_2$), 66.0 (d, area 2; P═S), −7.1 (d, area 1; $POP(O)(OH)_2$). $^{31}P\{^1H\}$ VT NMR ($CD_2Cl_2$) $^2J_{PNP}$, $^2J_{POP}$, Hz (temp, °C): 67.5, 20.6 (25); 67.1, 18.3 (0); 66.3, 16.6 (−20); 65.2, 12.6 (−40); 63.3, br (−60). $^1H$ NMR ($CD_2Cl_2$): δ 11.18 (br s, area 2; $P(OH)_2$), 7.42 (m, area 2; $C_6H_4$ ortho), 7.05 (m, area 2; $C_6H_4$ meta), 3.23 (m, area 16; $CH_2CH_3$), 1.18 (t, area 12; $CH_2CH_3$), 1.07 (t, area 12; $CH_2CH_3$). MS ($EI^+$), $M^+$ *m/e* (% rel int): 646 (3).

**Reactions of $C_6H_4N_2[P(NEt_2)_2]_2PCl$ (5) with ROH. $C_6H_4N_2[P(S)(NEt_2)_2]_2POR$ [R = Me (21), Et (22), i-Pr (23)].** **4** was combined with excess ROH (R = Me, Et, i-Pr, t-Bu) in $CH_2Cl_2$ at 25 °C. After 10 min, excess ROH and solvent were removed in vacuo, leaving products (**21**–**23**) as oils. **21** was isolated and fully characterized. $^{31}P\{^1H\}$ NMR ($CH_2Cl_2$): δ 108.9 (t, area 1, $^2J_{PNP}$ = 52.9 Hz; $POCH_3$), 66.8 (d, area 2; P═S). $^1H$ NMR ($C_6D_6$): δ 8.04 (m, area 2; $C_6H_4$ ortho), 6.94 (m, area 2; $C_6H_4$ meta), 3.28 (d, area 3, $^3J_{HP}$ = 7.8 Hz; $POCH_3$), 3.20 (m, area 16; $CH_2CH_3$), 1.07 (t, area 12, $^3J_{HH}$ = 7.08 Hz; $CH_2CH_3$), 0.95 (t, area 12, $^3J_{HH}$ = 7.08 Hz; $CH_2CH_3$). Mol wt: calcd for $C_{23}H_{47}N_6OP_3S_2$, 580.2466; found (EI+, exact mass), 580.2445. MS ($EI^+$), $M^+$ *m/e* (% rel int): 580 (8). **22** and **23** were characterized by $^{31}P\{^1H\}$ NMR as mixtures (with **8**): **22**, δ 108.2 (t, area 1, $^2J_{PP}$ = 53.3 Hz; $POCH_2CH_3$), 68.6 (d, area 2; P═S): **23**, δ 109.6 (t, area 1, $^2J_{PNP}$ = 59.4 Hz; $POCH(CH_3)_2$), 68.6 (d, area 2; P═S).

t-BuOH and **5** did not react.

**Variable-Temperature NMR Data. (A) $^{31}P$ NMR: 3–8, 9, and 11.** **3**–**8** exhibited characteristic $^{31}P\{^1H\}$ NMR $AX_2$ triplet–doublet spectral patterns over the temperature ranges studied. **3** (toluene-$d_8$, 24 °C): δ 106.5 [d, area 2; P(1), P(3)], 100.5 [t, area 1; P(2)]. $^2J_{PNP}$, Hz (temp, °C): 52.5 (104), 51.8 (84), 49.8 (54), 48.1 (30), 43.5 (27), 38.3 (−50), 34.4 (−70), 29.6 (−90). **4** (toluene-$d_8$, 27 °C): δ 65.1 [d, area 2; P(1), P(3)], 98.3 [t, area 1; P(2)]. $^2J_{PNP}$, Hz (temp, °C): 64.8 (105), 65.2 (90), 64.5 (60), 64.3 (30), 64.1(0), 64.1 (−30), 64.2 (−60), 64.3 (−94). **5** (toluene-$d_8$, 27 °C): δ 64.5 [d, area 2, $^2J_{PNP}$ = 66.7 Hz; P(1), P(3)], 143.9 [t, area 1; P(2)]. $^2J_{PNP}$, Hz (temp, °C): 64.1 (105), 64.5 (90), 65.7 (60), 66.1 (30), 66.5 (0), 67.5 (−30), 68.2 (−60), 68.4 (−90). **6** (toluene-$d_8$, 27 °C): δ 65.1 [d, area 2; P(1), P(3)], 94.1 [t, area 1; P(2)]. $^2J_{PP}$, Hz (temp, °C): 58.7 (100), 58.5 (40), 58.0 (−30), 57.0 (−60), 55.0 (−80), 53.5 (−90). **7** (toluene-$d_8$, 27 °C): δ 65.8 [d, area 2; P(1), P(3)], 121.4 [t, area 1; P(2)]. $^2J_{PNP}$, Hz (temp, °C): 70.7 (27), 71.5 (0), 72.5 (−60), 73.0 (−90). **8** (toluene-$d_8$, −27 °C): δ 111.9 [d, area 2; P(1), P(3)], 10.2 [t, area 1; P(1)]. $^2J_{PNP}$, Hz (temp, °C): 13.0 (100), 12.0 (40), 11.5 (0), 10.0 (−30), 8.5 (−60), 5.5 (−90). **9** (toluene-$d_8$, 121.2 MHz, +27 to −70 °C), resolved $AX_2$ pattern[19] (Figure 5A): δ 68.3 (t, area 1), 64.4 (d, area 2). $^2J_{PNP}$, Hz (temp, 0 °C): 20.6 (20), 21.0 (0), 21.4 (−20), 21.8 (−40), 21.8 (−50), 21.8 (−55), 22.2 (−60), 22.2 (−65), 22.5 (−70). The spectrum broadened below −70 °C; $T_c$ = −75 °C. By −110 °C the spectrum exhibited resonances from three conformers, **9A**–**C** (Figure 5B). **9A** (86% total spectral area), AMX pattern:[19] δ 68.5 (d of d, area 1, $^2J_{PNP}$ = 8.8 Hz, $^2J_{PNP}$ = 43.5 Hz), 63.0 (d, area 1), 62.4 (d, area 1). **9B** (13% total spectral area), $AX_2$ pattern: δ 65.5 (br t, area 1, $^2J_{PNP} \cong 7$ Hz), 63.8 (br d, area 2). **9C** (<1% total spectral area), $AX_2$ pattern: δ 70.5 (t, area 1, $^2J_{PNP} \cong 43$ Hz), 61.6 (d, area 2). **11** (toluene-$d_8$, +100 to −85 °C): $AX_2$ pattern. $^2J_{PNP}$(27 °C) = 14.7 Hz. $^{31}P\{^1H\}$ NMR (EtOH): at 27 °C, $AX_2$ pattern [$^2J_{PNP}$, Hz (temp, °C): 17.1 Hz (0), 17.6 (−30), 17.9 (−50), 18.0 (−60)]; at −70 to −90 °C, broad intermediate patterns, $T_c$ = −85 °C; at −110 °C, incompletely resolved ABX pattern, δ 18.6 (br m, area 1), 12.6 (br m, area 1), 10.0 (br m, area 1).

**(B) $^1H$ NMR: 4, 9, and 16.** **4** ($CD_2Cl_2$): spectrum temperature independent to −60 °C except for endo $CH_2CH_3$ resonances; endo $CH_2$ multiplet (∂ 2.86) observed, endo $CH_3$ resonances not resolved from other

**Table 1.** Crystal Data and Details of the Structure Determinations for **9**, **12**, and **16**

| | **9** | **12** | **16** |
|---|---|---|---|
| formula | $C_{26}H_{54}N_7P_3S_3$ | $C_{26}H_{54}N_7P_3Se_2$ | $C_{27}H_{57}N_7P_3S_2I$ |
| fw | 653.86 | 715.6 | 763.7 |
| space group | *Aba*2 | *Pbca* | $C222_1$ |
| crystal system | orthorhombic | orthorhombic | orthorhombic |
| *a*, Å | 23.111(4) | 14.975(6) | 10.885(4) |
| *b*, Å | 21.324(5) | 18.894(7) | 20.78(2) |
| *c*, Å | 14.609(3) | 24.524(8) | 36.31(2) |
| *V*, Å$^3$ | 7200(2) | 6939(3) | 8214(9) |
| *Z* | 8 | 8 | 8 |
| $d_{obs}$, g/cm$^3$ | 1.24 | 1.370 | 1.315 |
| $\mu$, cm$^{-1}$ | 3.60 | 2.083 | 1.012 |
| $\lambda$ (Mo K$\alpha$), Å | 0.710 73 | 0.710 69 | 0.710 73 |
| *T*, K | 295–297 | 193 | 295–297 |
| programs | SHELXTL | SHELXTL PLUS | SHELXTL |
| *R*, $R_w$ | 0.042, 0.045 | 0.053, 0.058 | 0.048, 0.05 |
| goodness of fit | 1.28 | 1.53 | 1.23 |

**Table 2.** Atomic Coordinates[a] (×10$^4$) and Equivalent Isotropic Displacement Parameters (Å$^2$ × 10$^3$) for $C_6H_4N_2[P(S)(NEt_2)_2]_2P(S)NEt_2$ (**9**)

| atom | *x* | *y* | *z* | $U_{eq}$[b] |
|---|---|---|---|---|
| S(1) | 2393(1) | 8806(1) | 1474(1) | 67(1)* |
| S(2) | 1046(1) | 7828(1) | 1084(1) | 67(1)* |
| S(3) | 1296(1) | 5838(1) | 3668(1) | 59(1)* |
| P(1) | 1875(1) | 8913(1) | 2501(1) | 45(1)* |
| P(2) | 1508(1) | 7599(1) | 2125(1) | 42(1)* |
| P(3) | 910(1) | 6402(1) | 2828(1) | 41(1)* |
| N(1) | 1632(1) | 8201(2) | 2903(2) | 40(1)* |
| N(2) | 1177(1) | 7151(2) | 2937(2) | 41(1)* |
| N(3) | 2165(2) | 9224(2) | 3432(2) | 47(1)* |
| N(4) | 1312(2) | 9344(2) | 2254(3) | 57(1)* |
| N(5) | 2107(2) | 7243(2) | 1868(3) | 57(1)* |
| N(6) | 221(1) | 6514(2) | 3070(3) | 45(1)* |
| N(7) | 982(2) | 6183(2) | 1753(3) | 48(1)* |
| C(1) | 1388(2) | 8059(2) | 3783(3) | 36(1)* |
| C(2) | 1143(2) | 7462(2) | 3805(3) | 38(1)* |
| C(3) | 906(2) | 7234(2) | 4600(3) | 47(2)* |
| C(4) | 899(2) | 7600(3) | 5371(3) | 61(2)* |
| C(5) | 1133(2) | 8200(2) | 5354(3) | 54(2)* |
| C(6) | 1379(2) | 8426(2) | 4560(3) | 49(2)* |
| C(31) | 2604(2) | 8867(2) | 3929(4) | 61(2)* |
| C(32) | 3230(2) | 8968(3) | 3655(5) | 88(3)* |
| C(33) | 2260(2) | 9910(2) | 3422(3) | 60(2)* |
| C(34) | 2194(3) | 10185(3) | 4359(4) | 112(3)* |
| C(41) | 854(3) | 9467(3) | 2936(4) | 78(2)* |
| C(42) | 317(3) | 9081(3) | 2793(6) | 124(4)* |
| C(43) | 1198(3) | 9588(3) | 1331(4) | 81(2)* |
| C(44) | 1323(4) | 10273(3) | 1223(5) | 133(4)* |
| C(51) | 2391(3) | 7303(3) | 944(4) | 94(3)* |
| C(52) | 2508(4) | 6731(3) | 485(6) | 147(4)* |
| C(53) | 2501(3) | 7058(4) | 2646(5) | 121(4)* |
| C(54)# | 3031(5) | 7248(6) | 2704(8) | 78(5)* |
| C(54′)# | 2880(8) | 6619(7) | 2644(11) | 127(8)* |
| C(61) | −108(2) | 7073(2) | 2789(4) | 66(2)* |
| C(62) | −458(2) | 7377(3) | 3518(5) | 88(3)* |
| C(63) | −133(2) | 5954(2) | 3292(4) | 64(2)* |
| C(64) | −229(2) | 5860(3) | 4297(4) | 79(2)* |
| C(71) | 512(3) | 6290(3) | 1097(4) | 79(2)* |
| C(72) | 649(4) | 6257(5) | 141(5) | 160(5)* |
| C(73) | 1399(2) | 5695(2) | 1506(4) | 62(2)* |
| C(74) | 1156(3) | 5035(3) | 1518(5) | 95(3)* |

[a] Atoms have occupancies of 1.0 except as marked with # above: C(54), 0.50; C(54′), 0.50. [b] For atoms marked with *, the equivalent isotropic *U* is defined as one-third of the trace of the orthogonalized $U_{ij}$ tensor.

$CH_3$ resonances; at −20 °C the $CH_2$ multiplet resonance broadens, at −80 °C two equal area 2 multiplets ($\delta$ 3.3 and $\delta$ 2.4) are seen; $T_c$ = −50 °C (Figure 6). **9** ($CD_2Cl_2$): spectrum temperature independent to −90 °C except for general broadening. **16** ($CD_2Cl_2$): spectrum temperature independent to −60 °C except for endo $CH_2CH_3$ resonances; endo $CH_3$ triplet observed at $\delta$ 1.36 ($^3J_{HH}$ = 7.0 Hz); $CH_2$ resonances not resolved from other $CH_2$ resonances; at −40 °C endo $CH_3$ resonance becomes two area 3 triplets, $\delta$ 1.31 and 1.40 ($^3J_{HH}$ = 6.7 Hz); $T_c$ = −13 °C; below −60 °C, general spectral broadening.

**Table 3.** Atomic Coordinates[a] (×10$^4$) and Equivalent Isotropic Displacement Parameters (Å$^2$ × 10$^3$) for $C_6H_4[P(Se)(NEt_2)_2]_2PNEt_2$ (**12**)

| atom | *x* | *y* | *z* | $U_{eq}$[b] |
|---|---|---|---|---|
| Se(1) | 114(1) | 934(1) | 2166(1) | 54(1)* |
| Se(2) | −1719(1) | 1149(1) | 5326(1) | 72(1)* |
| P(1) | −1220(2) | 931(1) | 2430(1) | 41(1)* |
| P(2) | −1568(2) | 488(1) | 3589(1) | 36(1)* |
| P(3) | −2438(2) | 1064(2) | 4596(1) | 47(1)* |
| N(1) | −1348(4) | 1138(4) | 3088(3) | 37(3)* |
| N(2) | −1821(4) | 1188(4) | 4034(3) | 40(3)* |
| N(3) | −1828(5) | 1538(4) | 2126(3) | 54(3)* |
| N(4) | −1675(4) | 137(4) | 2394(3) | 41(3)* |
| N(5) | −591(5) | 201(4) | 3795(4) | 61(4)* |
| N(6) | −2875(5) | 269(4) | 4522(3) | 49(3)* |
| N(7) | −3218(5) | 1668(4) | 4533(3) | 58(3)* |
| C(1) | −1174(6) | 1812(5) | 3322(5) | 44(4)* |
| C(2) | −1431(6) | 1842(6) | 3860(5) | 47(4)* |
| C(3) | −1300(7) | 2439(5) | 4179(4) | 52(4)* |
| C(4) | −908(7) | 3012(6) | 3923(6) | 66(5)* |
| C(5) | −645(7) | 2990(6) | 3384(7) | 79(6)* |
| C(6) | −771(7) | 2393(6) | 3074(5) | 58(5)* |
| C(31) | −1741(8) | 1574(6) | 1518(5) | 82(4) |
| C(32) | −1250(8) | 2206(7) | 1354(5) | 108(5) |
| C(33) | −2678(8) | 1806(6) | 2347(5) | 87(4) |
| C(34)# | −2890(13) | 2530(10) | 2278(9) | 83(8) |
| C(34′)# | −3270(28) | 2193(25) | 1981(19) | 66(17) |
| C(41) | −2657(6) | 82(5) | 2455(4) | 53(3) |
| C(42) | −2983(7) | −613(5) | 2675(4) | 60(3) |
| C(43) | −1238(6) | −477(5) | 2130(4) | 51(3) |
| C(44) | −1554(7) | −617(6) | 1556(4) | 68(3) |
| C(51)# | 294(19) | 683(12) | 3782(10) | 74(8) |
| C(52)# | 473(20) | 760(13) | 4373(12) | 95(11) |
| C(51′)# | 50(18) | 566(12) | 4154(10) | 31(9) |
| C(52′)# | 796(23) | 902(15) | 3847(10) | 52(11) |
| C(53) | −440(6) | −557(5) | 3807(4) | 45(3) |
| C(54) | 240(6) | −824(5) | 3402(4) | 62(3) |
| C(61) | −3569(6) | 146(5) | 4096(4) | 45(3) |
| C(62) | −4515(6) | 123(5) | 4300(4) | 58(3) |
| C(63) | −2461(7) | −404(6) | 4745(5) | 75(3) |
| C(64) | −2968(9) | −735(7) | 5160(6) | 126(6) |
| C(71) | −3602(7) | 1891(5) | 4008(4) | 65(3) |
| C(72) | −3690(9) | 2671(6) | 3948(5) | 107(5) |
| C(73) | −3860(8) | 1775(7) | 5026(5) | 95(4) |
| C(74) | −3587(8) | 2420(7) | 5318(5) | 113(5) |

[a] Atoms have occupancies of 1.0 except as marked with # above: C(34), 0.72; C(34′), 0.28; C(51), 0.58; C(52), 0.58; C(51′), 0.42; C(52′), 0.42. [b] For atoms marked with *, the equivalent isotropic *U* is defined as one-third of the trace of the orthogonalized $U_{ij}$ tensor.

**X-ray Analyses. (A) $C_6H_4N_2[P(S)(NEt_2)_2]_2P(S)NEt_2$ (9).** Crystallographic data were collected at −80 °C, because analysis of data collected at 25 °C showed significant disorder in the ethyl groups. Data collection and structure solution details are summarized in Table 1 and listed in the supplementary tables. The structure was solved by direct methods and refined by block-cascade least-squares calculations treating non-hydrogen atoms anisotropically. Hydrogen atoms were refined as fixed groups. Calculations were carried out using programs in the SHELXTL package. Metrical details are listed in the supplementary tables.

**(B) $C_6H_4N_2[P(Se)(NEt_2)_2]_2PNEt_2$ (12).** Crystallographic data were collected at −80 °C. Details of the data collection and structure solution are summarized in Table 1 and listed in the supplementary tables. The structure was solved by direct methods and refined by least-squares calculations. An empirical absorption correction was applied. All non-hydrogen atoms except the ethyl carbon atoms were treated anisotropically. The ethyl carbon atoms were treated isotropically, and the hydrogen atoms were included in idealized positions and refined riding on the atom to which they were attached. Calculations were carried out using programs in the SHELXTL package. Metrical details are listed in the supplementary tables.

**(C) $\{C_6H_4N_2[P(S)(NEt_2)_2]_2P(CH_3)NEt_2\}I$ (16).** Crystallographic data were collected at room temperature (22–24 °C). Details of the data collection and structure solution are summarized in Table 1 and listed in the supplementary tables. The toluene solvent molecule was disordered and included in multiple positions. The structure was solved by direct methods and refined by least-squares calculations treating non-hydrogen atoms anisotropically. Hydrogen atoms were included in idealized

**Table 4.** Atomic Coordinates[a] (×10⁴) and Equivalent Isotropic Displacement Parameters (Å² × 10³) for $\{C_6H_4N_2[P(S)(NEt_2)_2]_2P(CH_3)NEt_2\}I$ (**16**)

| atom | x | y | z | $U_{eq}$[b] |
|---|---|---|---|---|
| I(1)# | 5971(1) | 5000 | 5000 | 92(1)* |
| I(2)# | 0 | 4010(1) | 2500 | 112(1)* |
| P(1) | 2065(3) | 5398(1) | 3731(1) | 57(1)* |
| P(2) | 2688(2) | 3998(1) | 3707(1) | 42(1)* |
| P(3) | 1910(3) | 2624(1) | 3748(1) | 52(1)* |
| S(1) | 3721(3) | 5491(1) | 3552(1) | 73(1)* |
| S(2) | 3566(3) | 2499(1) | 3567(1) | 65(1)* |
| N(1) | 1834(8) | 4609(4) | 3872(2) | 43(3)* |
| N(2) | 1778(7) | 3421(3) | 3885(2) | 46(3)* |
| N(3) | 1727(11) | 5803(4) | 4103(2) | 78(4)* |
| N(4) | 1062(9) | 5576(5) | 3429(2) | 64(4)* |
| N(5) | 4043(7) | 3998(4) | 3873(2) | 46(3)* |
| N(6) | 1507(8) | 2239(3) | 4123(2) | 56(3)* |
| N(7) | 848(9) | 2468(4) | 3446(2) | 62(3)* |
| C(1) | 849(10) | 4374(5) | 4091(3) | 50(4)* |
| C(2) | 793(11) | 3692(5) | 4096(3) | 51(4)* |
| C(3) | −70(12) | 3403(6) | 4305(3) | 75(5)* |
| C(4) | −953(14) | 3765(8) | 4490(3) | 96(6)* |
| C(5) | −909(14) | 4417(7) | 4482(3) | 95(6)* |
| C(6) | −12(12) | 4721(6) | 4285(3) | 76(5)* |
| C(21) | 2676(9) | 3985(5) | 3226(2) | 53(3)* |
| C(31) | 2558(17) | 5700(6) | 4418(3) | 131(9)* |
| C(32) | 1991(19) | 5845(7) | 4785(3) | 196(12)* |
| C(33) | 1096(20) | 6428(8) | 4085(5) | 146(10)* |
| C(34) | 1792(21) | 6974(8) | 4093(6) | 208(13)* |
| C(41) | 1390(14) | 5714(8) | 3024(4) | 129(8)* |
| C(42) | 1296(20) | 6384(7) | 2933(5) | 172(11)* |
| C(43)# | −230(13) | 5635(12) | 3524(7) | 84(12)* |
| C(43′)# | −102(18) | 5236(12) | 3395(8) | 107(19)* |
| C(44)# | −897(45) | 5081(18) | 3333(10) | 147(22)* |
| C(44′)# | −1165(26) | 5572(13) | 3201(7) | 88(12)* |
| C(51) | 5163(10) | 3911(5) | 3649(3) | 81(5)* |
| C(52) | 6169(11) | 4369(6) | 3726(4) | 114(7)* |
| C(53) | 4185(10) | 4052(5) | 4276(2) | 66(4)* |
| C(54) | 4898(13) | 3485(5) | 4440(3) | 89(5)* |
| C(61) | 1176(13) | 1543(5) | 4089(3) | 78(5)* |
| C(62) | 2207(15) | 1097(7) | 4107(4) | 130(8)* |
| C(63) | 2205(12) | 2378(5) | 4462(3) | 72(5)* |
| C(64) | 1529(17) | 2175(6) | 4810(3) | 143(9)* |
| C(71) | −482(12) | 2492(8) | 3534(5) | 121(7)* |
| C(72) | −1178(15) | 3013(8) | 3379(4) | 144(8)* |
| C(73) | 1133(13) | 2350(6) | 3054(3) | 85(5)* |
| C(74) | 1117(16) | 1662(7) | 2955(4) | 130(8)* |
| C(91)# | 5000 | 4677(27) | 2500 | 69(16) |
| C(92)# | 5000 | 3616(27) | 2500 | 98(17) |
| C(93)# | 5000 | 2958(8) | 2500 | 125(17)* |
| C(94)# | 4260 | 3719 | 2379 | 287(34)* |
| C(95)# | 3644 | 4589 | 2326 | 174(24)* |
| C(96)# | 3549 | 3885 | 2317 | 95(14) |
| C(97)# | 4310 | 4293 | 2439 | 106(13)* |
| C(98)# | 4539 | 5039 | 2434 | 165(28)* |
| C(99)# | 3931 | 3223 | 2350 | 192(22)* |

[a] Atoms have occupancies of 1.0 except as marked with # above: I(1), 0.50; I(2), 0.50; C(43), 0.50; C(43′), 0.50; C(44), 0.50; C(44′), 0.50; C(91), 0.20; C(92), 0.22; C(93), 0.38; C(94), 0.68; C(95), 0.50; C(96), 0.40; C(97), 0.62; C(98), 0.47; C(99), 0.62. [b] For atoms marked with *, the equivalent isotropic $U$ is defined as one-third of the trace of the orthogonalized $U_{ij}$ tensor.

positions and refined riding on the atom to which they were attached. Calculations were carried out using programs in the SHELXTL package. Metrical details are listed in the supplementary tables.

## Results and Discussion

**Triphosphazane Reactions.** Reactions of **3**, oxidation by elemental sulfur, selenium, ozone, and phenyl azide or borane ($BH_3$) coordination, occur with high regioselectivity at the exo phosphorus positions. Only in reactions with $S_8$ and $O_3$ have trisubstituted products been obtained. Previously we reported that **3** reacts with $S_8$ in 10 min at 25 °C to form **4** quantitatively (eq 1, Scheme 1);[2b] only after **3**/$S_8$ reaction mixtures are heated in refluxing toluene for 48 h does oxidation at the central

**Scheme 1**

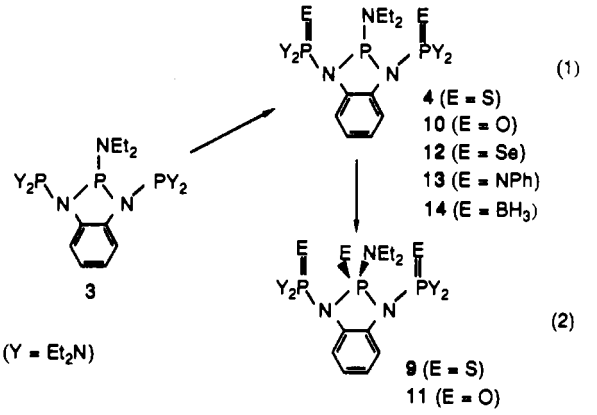


phosphorus occur to form **9** (eq 2). Ozone, the only [O] oxidizing agent of several we examined which would cleanly oxidize **3** to P=O bond containing products, reacts readily first at the exo and then more slowly at the endo phosphorus position. Here, reactions at the exo and endo positions are sufficiently close in rate that it was not possible to obtain the dioxide $C_6H_4N_2[P(O)(NEt_2)_2]_2PNEt_2$ (**10**) free of the trioxide $C_6H_4N_2[P(O)(NEt_2)_2]_2P(O)NEt_2$ (**11**). However, even though regioselectivity between endo and exo positions is small, there was no evidence for reaction first at the endo position. Examination of product mixtures by $^{31}P$ NMR analysis immediately after reaction onset and periodically during reaction showed no evidence for formation of endo monooxide or unsymmetrically substituted, endo–exo, dioxide products. In contrast, as with $S_8$, reactions of **3** with elemental Se, $PhN_3$, or $BH_3$·THF proceed easily to the exo-dioxidized or coordinated products $C_6H_4N_2[P(Se)(NEt_2)_2]_2PNEt_2$ (**12**), $C_6H_4N_2[P(NPh)(NEt_2)_2]_2PNEt_2$ (**13**), and $C_6H_4N_2[P(BH_3)(NEt_2)_2]_2PNEt_2$ (**14**), respectively. No monosubstituted products are seen. Even under more forcing conditions, no trisubstituted products form. The new triphosphazanes **11**–**14** exhibit the expected spectral characteristics. All show the expected mass spectral parent ions and $^{31}P$ NMR doublet resonances in regions characteristic of tris(amino)phosphine oxides,[27] selenides,[28] imines,[29] and boranes.[27,30-32] **14** displays a characteristic $^{11}B$ NMR resonance at $\delta$ −33.4.[31] The structures of **9** and **12** were also confirmed by single-crystal X-ray analysis (see below).

Selective reactivity at the triphosphazane endo phosphorus, apparently due to the size-restricted molecular cleft at that position, is seen further in $BH_3$ coordination and $CH_3I$ quaternization of **4**. **4** reacts slowly and incompletely with $B_2H_6$ or $BH_3$THF to form the endo-$BH_3$-substituted **15** (Scheme 2). Typically, reactions reach equilibrium in 15 min at 25 °C; these reactions contain both uncoordinated **4** and $BH_3$-coordinated **4**. Under vacuum, $BH_3$ can be removed from **15**, and **4** re-forms. **4** reacts slowly but quantitatively with $CH_3I$ to form the quaternary salt **16** (Scheme 2, eq 4). Because **15** is extensively dissociated in solution, its characterization is based on $^{31}P$ and $^{11}B$ NMR spectra of the adduct in solution. **15** and **16** show $^{31}P$ NMR doublet resonances at $\delta$ 66.4 and 65.7 characteristic of the exo $(amino)_3P{=}S$ groups.[27,33] The $BH_3$-coordinated endo phosphorus of **15** exhibits a broad $^{11}B$ NMR resonance at $\delta$ −51.8.

(27) Crutchfield, M. M.; Dungan, C. H.; Letcher, J. H.; Mark, V.; Van Wazer, J. R. *Topics in Phosphorus Chemistry*; Interscience: New York, 1963; Vol. 5.
(28) Kroshefsky, R. D.; Weiss, R.; Verkade, J. G. *Inorg. Chem.* **1979**, *18*, 469.
(29) Abel, E. W.; Mucklejohn, S. A. *Phosphorus Sulfur* **1981**, *9*, 235.
(30) Xi, S. K.; Schmidt, H.; Lensink, C.; Kim, S.; Wintergrass, L. M.; Daniels, L. M.; Jacobson, R. A.; Verkade, J. G. *Inorg. Chem.* **1990**, *29*, 2214.
(31) Kanjolia, R. K.; Srivastava, D. K.; Watkins, C. L.; Krannich, L. K. *Inorg. Chem.* **1989**, *28*, 2241.
(32) Rudolph, R. W.; Schultz, C. W. *J. Am. Chem. Soc.* **1971**, *93*, 6821.

**Scheme 2**

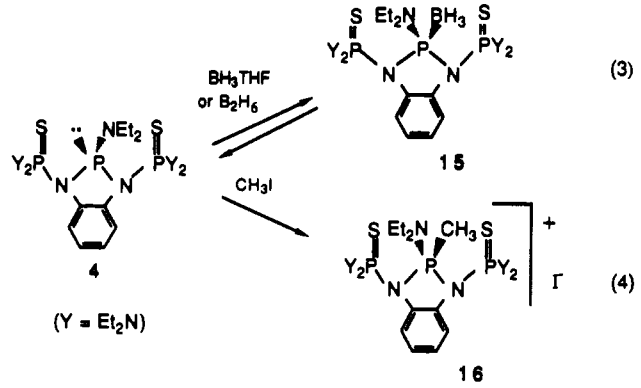


**Scheme 3**

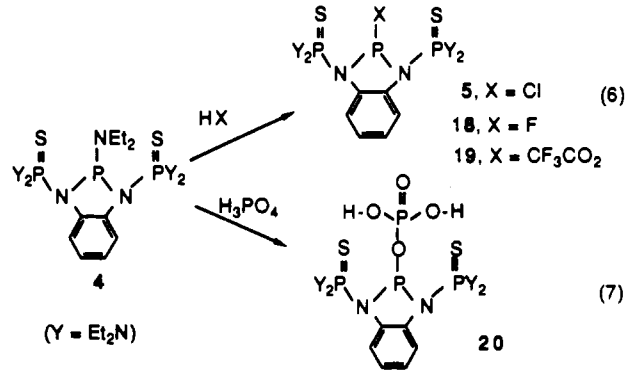


For **16**, the $^{31}P\{^{1}H\}$ NMR triplet resonance at $\delta$ 62.1 and the $^{1}H$ NMR area 3 $CH_3$ doublet resonance at $\delta$ 3.18 are as expected for a triphosphazane quaternized at the endo phosphorus. The structure of **16** has been confirmed also by single-crystal X-ray analysis (see below).

The **4**/$BH_3$ and **4**/$CH_3I$ reactions are of interest because both are suprisingly slow and from the **4**/$BH_3$ reaction there is evidence that the thermodynamic basicity of the endo phosphadiazole center is much lower than expected for tris(amino)phosphines.[34,35] Phosphines like $(Et_2N)_3P$ coordinate $BH_3$[34] or are quaternized[36,37] rapidly and quantitatively. The reactions have large equilibrium constants. That reactions with **4** are slower is consistent with the cleft at the endo phosphorus center being highly sterically restricted. The cleft appears barely large enough to allow entry of the $BH_3$ group or to accommodate the trigonal bipyamidal reaction intermediate which likely is involved in the quaternization process.[38] The low basicity of the endo phosphadiazole center is shown by the incomplete $BH_3$ coordination to **4**; at equilibrium at 25 °C both **15** and **4** are present. The experimentally determined equilibrum constant for the **4**/$BH_3$·THF reaction (in eq 5), as determined by integration of peak areas in the $^{31}P$ NMR

$$4 + BH_3\cdot THF \rightleftharpoons 4\cdot BH_3 + THF \qquad (5)$$

spectrum, is 15 ± 4. Suprisingly, the basicities of **4** and THF are comparable. Although equilibrium constants for other tris(amino)phosphine–borane association reactions appear unavailable, qualitatively such reactions generally go completely to isolable adducts.[34] It is not clear why basicity at the endo phosphorus of **4** is low; however, it may be due to electron-withdrawing properties of the two exo $(Et_2N)_2P(S)$ groups.

Derivatization of endo phosphorus centers in the skeletally stabilized phosphazanes is possible by replacement of $Et_2N$– or Cl–substituents of the triphosphazanes **4** and **5**. As with oxidation and Lewis acid coordination reactions, functional reagents need to be sterically relatively small. Reactions of **4** with protic acids, analogous to the **4**/HCl reaction reported earlier,[2b] occur easily with little evidence for cleavage of phosphazane P–N bonds (Scheme 3, eqs 6 and 7). **4** reacts with $CF_3CO_2H$ and $H_3PO_4$, cleaving the $Et_2N$– group and forming the new triphosphazanes **19** and **20**. **4** with $HBF_4$ in ether immediately yields the fluorotriphosphazane **18**. There is no evidence for intermediate phosphenium[39] tetrafluoroborate product formation, e.g. $\{C_6H_4N_2[P(S)(NEt_2)_2]_2P\}^{+}BF_4^{-}$. It was not possible to completely remove **18** and **19** from the accompanying ammonium salt products or **20** from the simultaneously formed $BF_3$·$Et_2NH$; nevertheless, **18**–**20** could be characterized unambiguously from spectral data obtained on the mixtures. Similarly, chlorotriphosphazane **5** reacts with alcohols MeOH and EtOH and slowly with i-PrOH, to form respectively the alkoxytriphosphazanes **21**–**23** (eq 8). Again, as with the amine/**5** reactions,[2b] only the

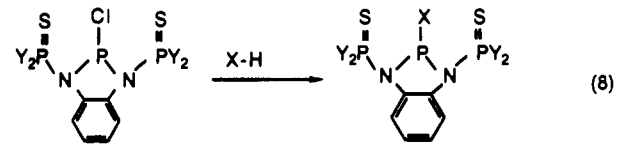


Y = $Et_2N$; X = MeO, **21**; EtO, **22**; i-PrO, **23**
" ; X = $Me_2N$, **24**; $Et_2N$, **25**; $(i\text{-}Pr)_2N$, **26**[2b]

sterically nonbulky alcohols react. Although i-PrOH reacts slowly, t-BuOH does not. $MeNH_2$, $EtNH_2$, and i-$PrNH_2$ react with **5** to form **24**–**26**, respectively; t-$BuNH_2$ does not react.[2b] **18**–**23** were obtained as uncrystallizable oils. All show characteristic $AX_2$ $^{31}P\{^{1}H\}$ NMR spectra consisting of area 2 doublet resonances[2b] between $\delta$ 66.8 and 68.6 and area 1 resonances due to the substituted endo phosphorus atoms. **19** and **21**–**23** show the triplets characteristic of endo-phosphorus-substituted triphosphazanes; **18** displays a doublet of triplets due to $^{1}J_{PF}$ coupling (1184 Hz). **20** exhibits a triplet of doublets due to $^{2}J_{POP}$ coupling (20.6 Hz) with the phosphorus of the phosphate substituent group. **4** and **5** derivatization reactions are relatively clean; the main impurity results from traces of water. The **4**/$H_3PO_4$ reactions, even after the $H_3PO_4$ is dried by treatment with $P_4O_{10}$, and the **5**/ROH reactions invariably show impurity quantities of the phosphine oxide $C_6H_4N_2[P(S)(NEt_2)_2]_2P(O)H$ (**8**).[2b]

The reduced reactivity at the central (endo) phosphorus of skeletally stabilized triphosphazanes **3**–**5** is similar to, but more pronounced than, that observed previously for the acyclic triphosphazane $Ph_2PN(Me)PPhN(Me)PPh_2$,[37] which in reaction with $S_8$ also showed regioselective formation of the exo disulfide $Ph_2P(S)N(Me)PPhN(Me)P(S)Ph_2$. Thus, the regioselectivity observed in **4** may not to be unique to the skeletally stabilized systems. It may be that reactivity of the internal P(III) atoms of higher oligomers or phosphazane polymers will in general be greatly lowered.

**Triphosphazane Structural Studies.** NMR and X-ray structural studies of selected triphosphazanes in solution and in the solid state allow structure confirmation and the determination of detailed conformational information. X-ray analyses of the triphosphazane disulfide **4** were reported earlier;[2b] we have now obtained data on three additional triphosphazanes, the diselenide $C_6H_4N_2[P(Se)(NEt_2)_2]_2PNEt_2$ (**12**), the trisulfide $C_6H_4N_2[P(S)$-

(33) Schmidpeter, A. Brecht, H. *Angew. Chem., Int. Ed. Engl.* **1967**, *6*, 945.
(34) (a) Nöth, H.; Vetter, H.-J. *Chem. Ber.* **1963**, *96*, 1298. (b) Holmes, R. R.; Carter, R. P., Jr. *Inorg. Chem.* **1963**, *2*, 1146.
(35) (a) Verkade, J. G. *Coord. Chem. Rev.* **1972/1973**, *9*, 1. (b) Reiss, J. G. *Phosphorus Sulfur* **1986**, *27*, 93. (c) Verkade, J. G.; King, R. W.; Heitsch, C. W. *Inorg. Chem.* **1964**, *3*, 884.
(36) Ewart, G.; Payne, D. S.; Porte, A. L.; Lane, A. P. *J. Chem. Soc.* **1962**, 3984.
(37) Keat, R.; Sim, W.; Payne, D. S. *J. Chem. Soc. A* **1970**, 2715.
(38) March, J. *Advanced Organic Chemistry*, 3rd ed.; John Wiley and Sons: New York, 1985.
(39) Cowley, A. H.; Kemp, R. A. *Chem. Rev.* **1985**, *85*, 367.

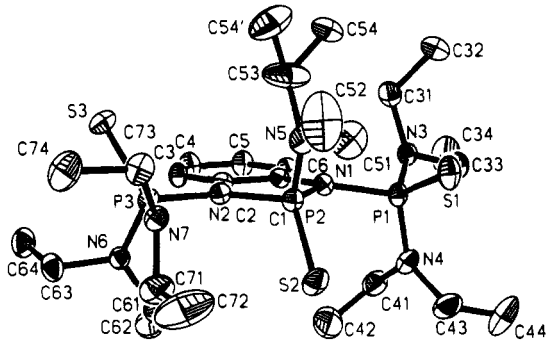


**Figure 1.** Structure and numbering scheme for $C_6H_4N_2[P(S)(NEt_2)_2]_2P(S)NEt_2$ (**9**). Thermal ellipsoids are shown at the 50% probability level. Hydrogen atoms are omitted for clarity.

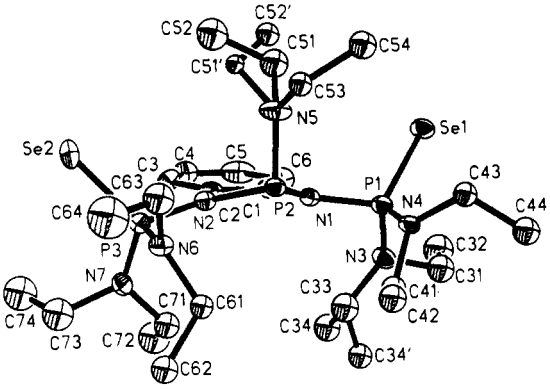


**Figure 2.** Structure and numbering scheme for $C_6H_4[P(Se)(NEt_2)_2]_2PNEt_2$ (**12**). Thermal ellipsoids are shown at the 50% probability level. Hydrogen atoms are omitted for clarity.

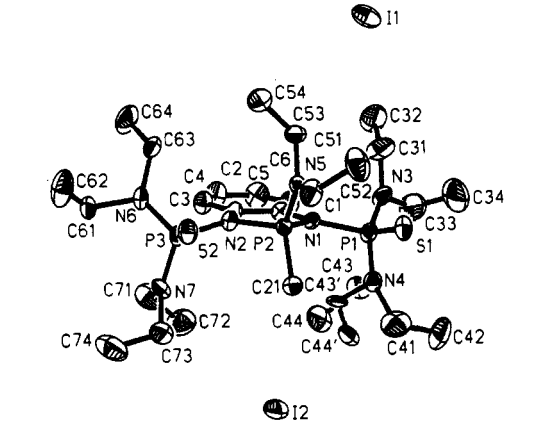


**Figure 3.** Structure and numbering scheme for $\{C_6H_4N_2[P(S)(NEt_2)_2]_2P(CH_3)NEt_2\}I$ (**16**). Thermal ellipsoids are shown at the 50% probability level. Hydrogen atoms are omitted for clarity.

$(NEt_2)_2]_2P(S)NEt_2$ (**9**), and the endo-methyl-quaternized $\{C_6H_4N_2[P(S)(NEt_2)_2]_2P(CH_3)NEt_2\}I$ (**16**). Compounds **4**, **9**, **12**, and **16** allow comparisons of the effects of exo substitutent size and endo group substitution on triphosphazane conformations. Finally, the conformations of these triphosphazanes in the solid state can be compared with those obtained by $^{31}P$ NMR spectroscopy in solution.

The structures of **9**, **12**, and **16** are shown in Figures 1–3. These can be compared with one another and with the previously reported triphosphazane disulfide $C_6H_4N_2[P(S)(NEt_2)_2]_2PNEt_2$ (**4**).[2b] **9** and **16**, as with **4**, adopt essentially symmetrical conformations in which the exo phosphorus P–E (E = S, Se, $CH_3$) groups and the P(2)–E,L groups (atom or lone-pair electrons) are on opposite sides of the $C_6N_2$ molecular plane. In all cases the $C_6N_2$ atoms are coplanar. The phosphadiazole phosphorus and the two exo phosphorus atoms are displaced in opposite directions from the $C_6N_2$ molecular plane, and these displacements depend strongly on whether the phosphadiazole phosphorus is $\lambda^3$ (as in **4** and **12**) or $\lambda^4$ (as in **9** and **16**) in type. In **9** and **16** the dihedral angles between the $C_6N_2$ and $N_2P$ planes [N(2)/P(3)/N)3)] are 2.7 and 3.7°, respectively. In contrast the analogous interplane angles in **4** and **12** are 21.2 and 21.4°. The P(1), P(2), and P(3) atom displacements from the $C_6N_2$ plane of **12** are –0.13, 0.47, and –0.37 Å. Consequently the P–N–P–N–P skeletal zigzag arrangement of the $\lambda^4$–$\lambda^3$–$\lambda^4$ sytems is greater than that of the $\lambda^4$–$\lambda^4$–$\lambda^4$ systems, a situation which would likely cause significant conformational differences if also expressed in oligomer or polymer chain systems.

The new triphosphazanes and the previously reported **4** have suprisingly similar structural parameters. Bond distances and angles are shown in Tables 5–7. In all cases, the mean exo (bonds to the phosphadiazole ring) and endo (bonds within the phosphadiazole ring) skeletal P–N distances are between 1.67 and 1.76 Å, in the range expected.[2,3,5,7,10,40–42] Differences in exo and endo P–N distances are noted, depending on the state of phosphorus oxidation; in **4** and **12**, which have only the outer two

**Table 5.** Selected Structural Parameters for $C_6H_4N_2[P(S)(NEt_2)_2]_2P(S)NEt_2$ (**9**)

(a) Distances, Å

| | | | |
|---|---|---|---|
| S(1)–P(1) | 1.933(2) | S(2)–P(2) | 1.922(2) |
| S(3)–P(3) | 1.938(2) | P(1)–N(1) | 1.723(4) |
| P(1)–N(3) | 1.655(4) | P(1)–N(4) | 1.633(4) |
| P(2)–N(1) | 1.738(3) | P(2)–N(2) | 1.704(3) |
| P(2)–N(5) | 1.622(4) | P(3)–N(2) | 1.718(3) |
| P(3)–N(6) | 1.649(4) | P(3)–N(7) | 1.647(4) |
| N(1)–C(1) | 1.436(5) | N(2)–C(2) | 1.433(5) |
| C(1)–C(2) | 1.395(6) | | |

(b) Angles, deg

| | | | |
|---|---|---|---|
| S(1)–P(1)–N(1) | 111.2(1) | S(1)–P(1)–N(3) | 115.7(1) |
| N(1)–P(1)–N(3) | 101.8(2) | S(1)–P(1)–N(4) | 112.9(2) |
| N(1)–P(1)–N(4) | 108.1(2) | N(3)–P(1)–N(4) | 106.2(2) |
| S(2)–P(2)–N(1) | 114.9(1) | S(2)–P(2)–N(2) | 116.3(1) |
| N(1)–P(2)–N(2) | 91.9(2) | S(2)–P(2)–N(5) | 114.2(1) |
| N(1)–P(2)–N(5) | 110.8(2) | N(2)–P(2)–N(5) | 106.4(2) |
| S(3)–P(3)–N(2) | 110.7(1) | S(3)–P(3)–N(6) | 113.5(2) |
| N(2)–P(3)–N(6) | 101.1(2) | S(3)–P(3)–N(7) | 112.4(1) |
| N(2)–P(3)–N(7) | 108.4(2) | N(6)–P(3)–N(7) | 110.1(2) |
| P(1)–N(1)–P(2) | 118.8(2) | P(1)–N(1)–C(1) | 128.2(3) |
| P(2)–N(1)–C(1) | 111.4(3) | P(2)–N(2)–P(3) | 128.1(2) |
| P(2)–N(2)–C(2) | 112.4(3) | P(3)–N(2)–C(2) | 119.4(3) |
| P(2)–N(5)–C(51) | 122.7(4) | P(2)–N(5)–C(53) | 117.6(4) |
| C(51)–N(5)–C(53) | 115.7(4) | | |

**Table 6.** Selected Structural Parameters for $C_6H_4N_2[P(Se)(NEt_2)_2]_2PNEt_2$ (**12**)

(a) Distances, Å

| | | | |
|---|---|---|---|
| Se(1)–P(1) | 2.100(3) | Se(2)–P(3) | 2.096(3) |
| P(1)–N(1) | 1.671(8) | P(1)–N(3) | 1.644(8) |
| P(1)–N(4) | 1.651(8) | P(2)–N(1) | 1.768(8) |
| P(2)–N(2) | 1.755(8) | P(2)–N(5) | 1.639(8) |
| P(3)–N(2) | 1.676(8) | P(3)–N(6) | 1.649(8) |
| P(3)–N(7) | 1.641(8) | N(1)–C(1) | 1.420(12) |
| N(2)–C(2) | 1.432(13) | C(1)–C(2) | 1.375(15) |

(b) Angles, deg

| | | | |
|---|---|---|---|
| Se(1)–P(1)–N(1) | 114.0(3) | Se(1)–P(1)–N(3) | 112.7(3) |
| N(1)–P(1)–N(3) | 102.3(4) | Se(1)–P(1)–N(4) | 112.2(3) |
| N(1)–P(1)–N(4) | 102.6(4) | N(3)–P(1)–N(4) | 112.3(4) |
| N(1)–P(2)–N(2) | 87.0(3) | N(1)–P(2)–N(5) | 106.1(4) |
| N(2)–P(2)–N(5) | 104.5(4) | Se(2)–P(3)–N(2) | 114.2(3) |
| Se(2)–P(3)–N(6) | 111.6(3) | N(2)–P(3)–N(6) | 104.9(4) |
| Se(2)–P(3)–N(7) | 113.1(3) | N(2)–P(3)–N(7) | 102.6(4) |
| N(6)–P(3)–N(7) | 109.9(4) | P(1)–N(1)–P(2) | 122.0(4) |
| P(1)–N(1)–C(1) | 125.4(6) | P(2)–N(1)–C(1) | 112.1(6) |
| P(2)–N(2)–P(3) | 121.6(4) | P(2)–N(2)–C(2) | 112.2(6) |
| P(3)–N(2)–C(2) | 126.2(7) | P(2)–N(5)–C(51′) | 127.6(11) |
| P(2)–N(5)–C(51) | 122.9(10) | C(51)–N(5)–C(53) | 115.5(11) |
| P(2)–N(5)–C(53) | 118.2(6) | C(51)–N(5)–C(51′) | 37.8(13) |
| C(51′)–N(5)–C(53) | 110.4(11) | | |

**Table 7.** Selected Structural Parameters for $\{C_6H_4N_2[P(S)(NEt_2)_2]_2P(CH_3)NEt_2\}I$ (**16**)

(a) Distances, Å

| | | | |
|---|---|---|---|
| P(1)–S(1) | 1.926(5) | P(1)–N(1) | 1.735(8) |
| P(1)–N(3) | 1.633(9) | P(1)–N(4) | 1.592(10) |
| P(2)–N(1) | 1.685(8) | P(2)–N(2) | 1.683(8) |
| P(2)–N(5) | 1.594(8) | P(2)–C(21) | 1.747(8) |
| P(3)–S(2) | 1.936(4) | P(3)–N(2) | 1.735(8) |
| P(3)–N(6) | 1.640(9) | P(3)–N(7) | 1.625(9) |
| N(1)–C(1) | 1.420(13) | N(2)–C(2) | 1.434(14) |
| N(5)–C(51) | 1.477(13) | N(5)–C(53) | 1.474(11) |
| C(1)–C(2) | 1.419(15) | | |

(b) Angles, deg

| | | | |
|---|---|---|---|
| S(1)–P(1)–N(1) | 109.3(3) | S(1)–P(1)–N(3) | 115.9(4) |
| N(1)–P(1)–N(3) | 102.1(4) | S(1)–P(1)–N(4) | 112.7(4) |
| N(1)–P(1)–N(4) | 108.9(5) | N(3)–P(1)–N(4) | 107.2(5) |
| N(1)–P(2)–N(2) | 94.4(4) | N(1)–P(2)–N(5) | 112.1(4) |
| N(2)–P(2)–N(5) | 113.5(4) | N(1)–P(2)–C(21) | 111.3(4) |
| N(2)–P(2)–C(21) | 111.6(5) | N(5)–P(2)–C(21) | 112.7(4) |
| S(2)–P(3)–N(2) | 107.6(3) | S(2)–P(3)–N(6) | 117.7(3) |
| N(2)–P(3)–N(6) | 101.8(4) | S(2)–P(3)–N(7) | 114.0(4) |
| N(2)–P(3)–N(7) | 109.0(4) | N(6)–P(3)–N(7) | 105.9(4) |
| P(1)–N(1)–P(2) | 121.8(5) | P(1)–N(1)–C(1) | 126.8(7) |
| P(2)–N(1)–C(1) | 110.8(6) | P(2)–N(2)–P(3) | 121.4(5) |
| P(2)–N(2)–C(2) | 111.3(6) | P(3)–N(2)–C(2) | 126.2(7) |
| P(2)–N(5)–C(51) | 123.7(6) | P(2)–N(5)–C(53) | 118.2(6) |
| C(51)–N(5)–C(53) | 118.0(8) | | |

phosphorus atoms oxidized, the endo distances are ca. 1.67 Å, significantly shorter than the exo distances of 1.75–1.76 Å. In contrast, in **9**, where all phosphorus atoms are oxidized, the endo and exo distances are closely similar at 1.72 Å. The mean exo P–N–P angles are between 121.8 and 123.4°, as expected; the angles in **9** are not significantly larger than those in **4** and **12**. Apparently, the presence of the extra S atom or $CH_3$ group in the molecular cleft does not crowd the molecule enough to cause a widening of these bond angles. However, the individual angles P(1)–N(1)–P(2) and P(2)–N(2)–P(3) in **9** of 118.8 and 128.1° are quite different. This situation, which is not seen in **4** and **12**, may arise because the molecule adopts a twisted, unsymmetrical conformation in the solid state (see below).

The triphosphazane conformations, especially the orientation of P–E/P–L (E = bonded groups, atoms; L = lone-pair electrons) groups relative to one another and to the phosphazane P–N skeleton, can be compared. In order to define and easily compare conformations, individual group orientations are designated in terms of a dihedral angle $\theta$ (+ angle above and – angle below the horizontal plane) between the plane which contains the P–E/P–L vector and the group's adjacent $P_2N$ plane (Figure 4A). The molecule is oriented such that the $C_6N_2$ plane is horizontal, with the phosphorus atoms forward. For two P–E/P–L groups relative to a given $P_2N$ plane (one P–E group on each side), two angles, $\theta$ and $\theta'$, are given; e.g., a diphosphazane $[(RP)_2NR']$ conformation where the P–L vectors are "cis" and coplanar with the $P_2N$ molecular plane is defined as (in deg) $\theta = \theta' = 0$. In order to define orientations of the three P–E groups of the triphosphazanes **4**, **9**, **12**, and **16**, four angles are used: $\theta_1, \theta_1', \theta_2, \theta_2'$. This approach is preferable to more qualitative designations or to one where angles are defined relative to some "average" molecular plane, since the degrees to which phosphorus atoms lie away from the $C_6N_2$ molecular planes vary widely. Intervector angles, i.e. angles between adjacent pairs of P–E or P–L groups, are given by $\Theta$, which is the sum $|\theta| + |\theta'|$, as an angle less than 180°. The P–E group orientations around each $P_2N$ plane in **4**, **9**, **12**, and **16**, viewed down the P(3)···P(2) and P(2)···P(1) vectors, are shown in Figure 4B–E.

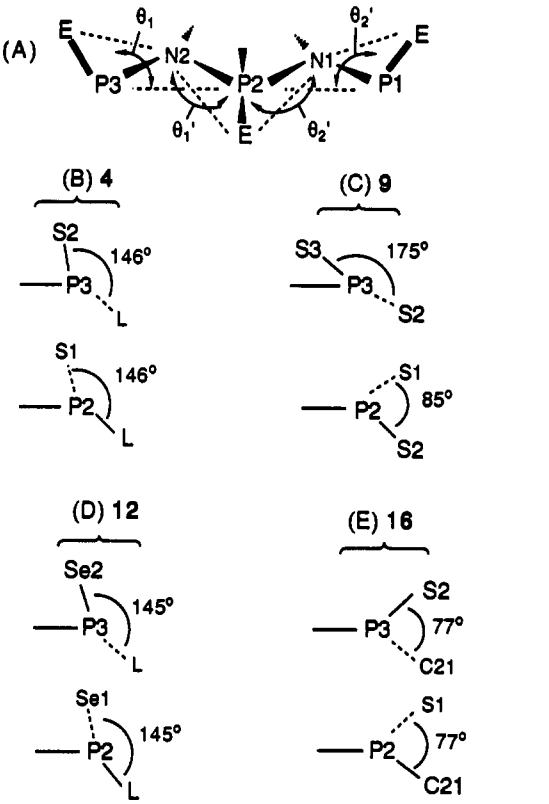


**Figure 4.** Dihedral angle relationships in triphosphazanes: (A) definition of $\theta$ and $\theta'$; (B–D) dihedral angles between the P(3)-E and P(2)-E,L groups as viewed down the P(3)···P(2) and P(2)–E and P(1)–E vectors in **4**, **9**, **12**, and **16**.

**Table 8.** Conformational Angles in **4**, **9**, **12**, and **16**

| | interplane angles,[a] deg | | | | inter P–E/P–L angles,[b] deg | |
|---|---|---|---|---|---|---|
| compd | $\Theta_1$ | $\Theta_1'$ | $\Theta_2$ | $\Theta_2'$ | $\Theta_1$ | $\Theta_2$ |
| **4** | 106 | –40 | –37 | 109 | 146 | 146 |
| **9** | 120 | –64 | –50 | 35 | 175 | 85 |
| **12** | 110 | –35 | –42 | 103 | 145 | 145 |
| **16** | 25 | –52 | –53 | 24 | 77 | 77 |

[a] Dihedral angle between P–E/P–L group vector and adjacent $P_2N$ plane; + and – refer to angles above and below the $P_2N$ plane, respectively. [b] Angle between P–E/P–L groups on adjacent phosphorus atoms.

The $\theta$ and $\Theta$ conformational angles in **4**, **9**, **12**, and **16** are given in Table 8. Because of the structural constraints imposed on the central phosphadiazole phosphorus, its P–E or P–L group always has a negative $\theta$ angle in the range –35 to –64°. **4**, **12**, and **16** are within experimental error symmetrical; in all cases the orientations of the exo P–E groups relative to the central P–S (or P–L) unit are close to equal (Figure 4B,D,E). The P═S and P═Se groups of **4** and **12** are close to trans oriented relative to the central P–L (Figure 4B,D) with $\Theta$ values ranging from 140 to 146°. The $\Theta$ angles in **4** and **12** are remarkably similar, even though van der Waals radii of S (1.80 Å) and Se (1.90 Å)[43] are somewhat different. Seemingly, the triphosphazane skeletal conformation is insensitive to relatively small changes in the exo P–E groups, a result which might be important to higher phosphazane and polyphosphazane conformational properties. In **16**, the P═S bonds are rotated forward and are approximately orthogonal to the P–L units (Figure 4E; $\Theta_1 = \Theta_2 = 77°$). In contrast to the situtation in **4**, **12**, and **16**, the trisulfide **9** adopts an unsymmetrical conformation (Figure 4C) in which $\Theta_1$ and $\Theta_2$ angles are 175 and 85°, respectively. How the conformations are determined by the particular groups present in a given

(40) Zeiss, W.; Schwarz, W.; Hess, H. *Angew. Chem., Int. Ed. Engl.* **1977**, *16*, 407.
(41) Gallicano, K. D.; Paddock, N. L. *Can. J. Chem.* **1985**, *63*, 314.
(42) Shaw, R. A. *Phosphorus Sulfur* **1978**, *4*, 101.
(43) Powell, P.; Timms, P. *The Chemistry of the Non-Metals*; Chapman and Hall: London, 1974.

triphosphazane is not clear; however, as more data are collected, this aspect of triphosphazane structural chemistry will be examined further.

The $^{31}P$ NMR spectra of selected triphosphazanes were examined as a function of temperature in order to obtain information about the conformational properties of the molecules in solution, barriers to rotation around the P–N skeletal bonds, and the extent to which the conformational properties are affected by substituents in the molecular cleft. The triphosphazanes examined were the parent triphosphazane **3**, the disulfide series $C_6H_4N_2[P(S)(NEt_2)_2]_2PX$ [**4**, X = $NEt_2$; **5**, X = Cl; **6**, X = $NH_2$; **7**, X = $N_3$; **8**, X = H(O); X = $OP(O)(OH)_2$, **20**], the diadduct $C_6H_4N_2[P(BH_3)(NEt_2)_2]_2PNEt_2$ (**14**), the diselenide **12**, the trioxidized series $C_6H_4N_2[P(E)(NEt_2)_2]_2P(E)NEt_2$ (**11**, E = O; **9**, E = S), and $\{C_6H_4N_2[P(S)(NEt_2)_2]_2P(CH_3)NEt_2\}I$ (**16**). These were selected because they are representative of the various classes, and because they could be obtained pure, reliable NMR data could be obtained.

Triphosphazane **3**, disulfide **4**, and diselenide **12** and disulfide derivatives **5–8**, **14**, **16**, and **20** all show their characteristic spectral patterns over the entire temperature ranges studied. All were examined from above ambient temperature (70–105 °C) down to −90 °C. **7**, an azide, was examined only between +25 and −90 °C. The $^2J_{PNP}$ values observed for the $\lambda^3$–$\lambda^3$–$\lambda^3$ (**3**), $\lambda^4$–$\lambda^3$–$\lambda^4$ (**4–7**, **12**, **14**, **20**), and $\lambda^4$–$\lambda^4$–$\lambda^4$ (**8**, **9**, **11**, **16**) series are consistent with those seen for analogous unsymmetrical diphosphosphazanes,[9–19] especially those which contain bulky substitutents.[9,11,12] The absolute $^2J_{PNP}$ values (the signs of $^2J_{PNP}$ were not determined) in all but **3** and **8** are nearly temperature independent, varying in general by less than 10% over the temperature range studied. This indicates that essentially unrestricted rotation occurs around skeletal P–N bonds over the range studied and that the conformational population is not very affected by temperature. Barriers to rotation ($\Delta G^*$) around P–N bonds are in the range expected for sterically unrestricted acyclic phosphazanes.[44–47] In **3** and **8** between +105 and −90 °C the $^2J_{PNP}$ values decrease from 52.5 to 29.6 Hz and from 13.0 to 5.5 Hz, respectively. It has been established previously that (i) $^2J_{PNP}$ couplings depend on the rotational angle around the P–N–P bond,[10,12,13,18,19] (ii) acyclic diphosphosphazanes adopt one of two conformations in which the phosphorus lone-pair electrons are either mutually cis or are in a trans arrangement,[9–12] and (iii) the trans conformation is favored by systems with large substituents on the skeletal phosphorus and nitrogen atoms.[9,12,14] Generally, for a given diphosphazane type, e.g. P(III)–P(III) or P(III)–P(V), the cis and trans conformations are associated with relatively larger and smaller $^2J_{PNP}$ values, respectively.[10,12,48] Thus, for the triphosphazanes studied here we conclude that conformations analogous to those seen in the solid state predominate in solution. For **3** and **8**, where $^2J_{PNP}$ decreases with temperature, it seems likely that the trans:cis conformation ratio increases slightly as the temperature is decreased.

In contrast to the other triphosphazanes studied, the trisulfide **9** and trioxide **11** show restricted P–N bond rotation around exo P–N bonds at low temperatures. The $^{31}P$ NMR spectrum of **9** as a function of temperature is shown in Figure 5. Both **9** (Figure 5A) and **11** display $AX_2$ spectra at 25 °C. Upon cooling, multiplet broadening followed by peak collapse occurs and the spectra undergo transitions to complex patterns, which in the case of **9** is clearly the result of a mixture of conformers. **9** undergoes coalesence ($T_c$) at −75 °C, which gives an activation barrier $\Delta G^*$

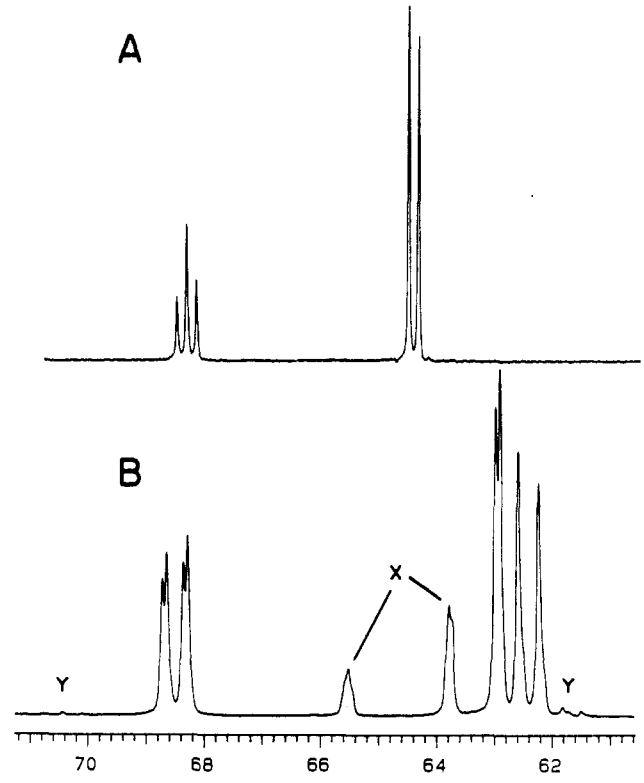


**Figure 5.** $^{31}P\{^1H\}$ NMR spectra of $C_6H_4N_2[P(S)(NEt_2)_2]_2P(S)NEt_2$ (**9**) at (A) 27 °C and (B) −110 °C. In spectrum B, major features are from **9A**; minor features from **9B** and **9C** are at *x* and *y*, respectively.

of 39.7 kJ/mol.[49,50] The spectrum of **11** is not sufficiently resolved at low temperature to allow a detailed assignment; hence, only an estimated coalesence temperature of ca. −75 °C was obtained. At −110 °C (Figure 5B), **9** exhibits resonances attributable to three conformers, **9A–C** in an 87:13:<1 mole ratio. **9A** gives an

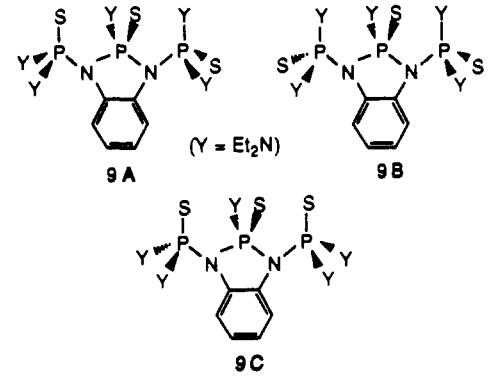


AMX type spectrum in which the three phosphorus atoms are inequivalent; the $^2J_{PNP}$ couplings between the endo and exo phosphorus atoms are 8.8 and 43.5 Hz. In contrast, **9B** and **9C** give $AX_2$ patterns characteristic of more highly symmetrical structures. **9B** and **9C** display $^2J_{PNP}$ values of 7 and 43 Hz, respectively.

Assuming we can correlate the $^2J_{PNP}$ values with approximate conformations around P–N–P bond units, we can suggest possible structures for **9A–C**. **9A**, would have one exo $P(S)(NEt_2)_2$ group rotated such that the exo and endo P=S bonds are approximately trans and the other $P(S)(NEt_2)_2$ group rotated such that they are in cis orientations. **9B** and **9C** would be symmetrical, **9B** with both exo P=S bonds trans to the endo P=S bond and **9C** with

(44) Cowley, A. H.; Dewar, M. J. S.; Jackson, W. R. *J. Am. Chem. Soc.* **1968**, *90*, 4185.
(45) DiStefano, S.; Goldwhite, H.; Mazzola, E. *Org. Magn. Reson.* **1974**, *6*, 1.
(46) Burdon, J.; Hotchkiss, J. C.; Jennings, W. B. *J. Chem. Soc., Perkin Trans. 2* **1976**, 1052.
(47) Dakternieks, D.; DiGiacomo, R. *Phosphorus Sulfur* **1985**, *24*, 217.
(48) Simonnin, M.-P.; Lequan, R.-M.; Wehrli, F. W. *J. Chem. Soc., Chem. Commun.* **1972**, 1204.
(49) Sandstrom, J. *Dynamic NMR Spectroscopy*; Academic Press: London, 1982.
(50) Kost, D.; Carlsen, E. H.; Raban, M. *Chem. Commun.* **1971**, 656.

both P=S bonds cis to the center endo bond. The proposed conformation for **9A** would be closely similar to what is seen in the solid state and is consistent with the fact that the lowest energy conformation for both **9** and **11** may be the same in the solid state as it is in solution.

Examination of the $^1$H NMR spectra of **4** and **16** as a function of temperature provides insight into the conformational restrictions that exist for the $(CH_3CH_2)_2N$ group in the triphosphazane molecular cleft. In addition, the effect on conformation of steric bulk in the cleft can be probed. Except for the endo $(CH_3CH_2)_2N$ group resonances, the $^1$H spectral resonances are temperature independent down to −90 °C. Because of spectral overlaps between $(CH_3CH_2)_2N$ group and other resonances, it was advantageous to observe the endo $(CH_3CH_2)_2N$ methyl ($CH_3$) resonances of **16** and the methylene ($CH_2$) resonance of **4**. The $(CH_3CH_2)_2N$ $CH_3$ resonance of **16** between 25 and −40 °C is shown in Figure 6. At 25 °C (Figure 6A) one area 6 triplet due to endo $CH_3$ groups ($\delta$ 1.38; $^3J_{HP}$ = 7.1 Hz) is observed. As the temperature is lowered, the triplet broadens (Figure 6B) and coalescence occurs (Figure 6C; $T_c$ = −13 °C). Further cooling yields two area 3 triplets ($\delta$ 1.31 and 1.40) (Figure 6D). At low temperatures the exo $(CH_3CH_2)_2N$ and P–$CH_3$ methyl resonances are unchanged. The endo $(CH_3CH_2)_2N$ $CH_2$ resonance of **4** between 0 and −90 °C goes from one complex multiplet to two distinct equal-area multiplets ($\delta$ 3.30 and 2.40) ($T_c$ = −50 °C). At −90 °C the exo $(CH_3CH_2)_2N$ resonances of **16** are generally broadened but otherwise unchanged. Barriers to rotation around the phosphadiazole exo P–N bond in **4** and **16** are calculated to be 42.3 and 54.5 kJ/mol, respectively.

The observed barriers to rotation around the endo $(CH_3CH_2)_2N$ phosphorus–nitrogen bonds in **4** and **16** differ measurably but are in the range of those observed for other $R_2N$-substituted phosphadiazoles. In the $C_6H_4(NMe)_2P$–$NR_2$ series, barriers of 38.0, 45.1, and 54.3 kJ/mol for the $NMe_2$, $NEt_2$, and N-i-$Pr_2$ derivatives, respectively, were measured.[51] It would be of interest to compare the endo $(CH_3CH_2)_2N$ group rotational properties of **4** and **16** with those of **9**, which contains a sulfur on phosphorus in the cleft. However, because restricted rotation around exo P–N bonds becomes significant as the temperature is lowered, general $^1$H spectral broadening occurs and detailed $^1$H spectral analysis is not possible. The higher barriers observed for **9** and **16** might be attributed to the additional S atom or $CH_3$ group in the molecular cleft. The barrier in **16** is higher than that in **4**, consistent with the fact that the effective size of a $CH_3$ group is larger than that of a S atom (van der Waals radii: $CH_3$, 4.6 Å; S, 3.6 Å).[43] Because two distinct $CH_3$ or $CH_2$ resonances are seen in the "frozen" state, it follows that the $CH_3CH_2$ groups are not located symmetrically relative to the main molecular plane but are oriented such that they become inequivalent. Such a conformation is approximately assumed by the endo $(CH_3CH_2)_2N$ groups in **4** and **16** in the solid state, so we suggest that this might be the lowest energy conformation for the endo $(CH_3CH_2)_2N$ group in the triphosphane systems. The R groups of the $C_6H_4(NMe)_2PNR_2$ series are also inequivalent in the frozen state;[51] hence this property appears unrelated to triphosphazane molecular cleft chacteristics.

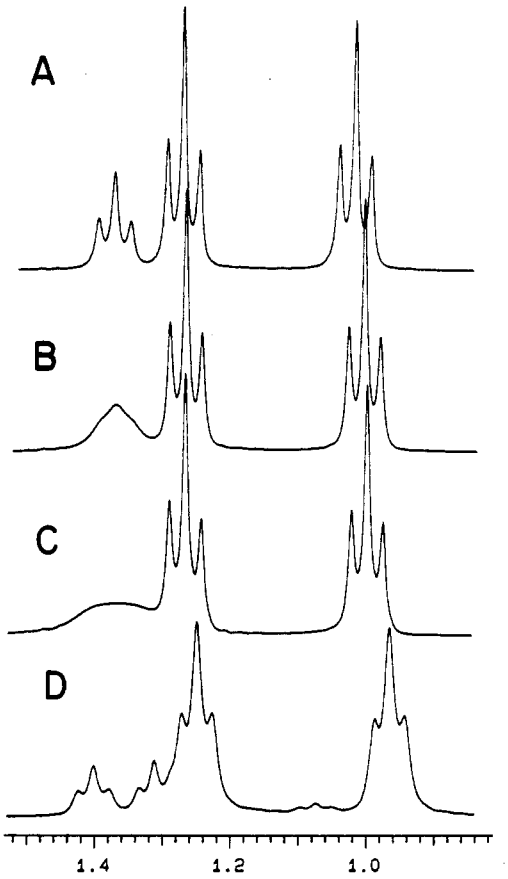


**Figure 6.** $^1$H NMR spectra of the $(CH_3CH_2)_2N$ methyl groups of $\{C_6H_4N_2[P(S)(NEt_2)_2]_2P(CH_3)NEt_2\}I$ (**16**) at (A) 25 °C, (B) 0 °C, (C) −13 °C, and (D) −40 °C.

**Acknowledgment.** We gratefully acknowledge support of this work by National Science Foundation Grants CHE 8312856 and CHE 8714951 and the donors of the Petroleum Research Fund, administered by the American Chemical Society.

**Supplementary Material Available:** Tables of crystal data and refinement details, anisotropic thermal parameters, hydrogen atom positions, complete bond distances and angles, and least squares planes (38 pages). Ordering information is given on any current masthead page.

(51) Jennings, W. B.; Randall, D.; Worley, S. D.; Hargis, J. H. *J. Chem. Soc., Perkin Trans. 2* **1981**, 1411.